https://doi.org/10.5194/gmd-2019-375
Preprint. Discussion started: 21 January 2020

Geoscientific Model Development Discussions

Reduced complexity model intercomparison project phase 1: Protocol, results and initial observations

Zebedee R. J. Nicholls[1,2], Malte Meinshausen[1,2,3], Jared Lewis[1], Robert Gieseke[3], Dietmar Dommenget[4], Kalyn Dorheim[5], Chen-Shuo Fan[4], Jan S. Fuglestvedt[6], Thomas Gasser[7], Ulrich Golüke[8], Philip Goodwin[9], Elmar Kriegler[3], Nicholas J. Leach[10], Davide Marchegiani[4], Yann Quilcaille[7], Bjørn H. Samset[6], Marit Sandstad[6], Alexey N. Shiklomanov[5], Ragnhild B. Skeie[6], Christopher J. Smith[11], Katsumasa Tanaka[12,13], Junichi Tsutsui[14], and Zhiang Xie[4]

[1]Australian–German Climate and Energy College, The University of Melbourne, Parkville, Victoria, Australia
[2]School of Earth Sciences, The University of Melbourne, Parkville, Victoria, Australia
[3]Potsdam Institute for Climate Impact Research (PIK), Member of the Leibniz Association, Potsdam, Germany
[4]Monash University, School of Earth, Atmosphere and Environment, Clayton, Victoria 3800, Australia
[5]Joint Global Change Research Institute, Pacific Northwest National Laboratory, College Park, MD, USA
[6]CICERO Center for International Climate Research, Oslo, Norway
[7]International Institute for Applied Systems Analysis (IIASA), Laxenburg, Austria
[8]BI Norwegian Business School, Nydalsveien 37, 0484 Oslo, Norway
[9]School of Ocean and Earth Science, University of Southampton, Southampton, UK
[10]Department of Physics, Atmospheric Oceanic and Planetary Physics, University of Oxford, United Kingdom
[11]Priestley International Centre for Climate, University of Leeds, UK
[12]National Institute for Environmental Studies (NIES), Tsukuba, Japan
[13]Laboratoire des Sciences du Climat et de l'Environnement (LSCE), Commissariat à l'énergie atomique et aux énergies alternatives (CEA), Gif sur Yvette, France
[14]Central Research Institute of Electric Power Industry, Abiko, Japan

Correspondence: Zebedee Nicholls (zebedee.nicholls@climate-energy-college.org)

Abstract.

Here we present results from the first phase of the Reduced Complexity Model Intercomparison Project (RCMIP). RCMIP is a systematic examination of reduced complexity climate models (RCMs), which are used to complement and extend the insights from more complex Earth System Models (ESMs), in particular those participating in the Sixth Coupled Model Intercomparison Project (CMIP6). In Phase 1 of RCMIP, with 14 participating models namely ACC2, AR5IR (2 and 3 box versions), CICERO-SCM, ESCIMO, FaIR, GIR, GREB, Hector, Held et al. two layer model, MAGICC, MCE, OSCAR and WASP, we highlight the structural differences across various RCMs and show that RCMs are capable of reproducing global-mean surface air temperature (GSAT) changes of ESMs and historical observations. We find that some RCMs are capable of emulating the GSAT response of CMIP6 models to within a root-mean square error of 0.2°C (of the same order of magnitude as ESM internal variability) over a range of scenarios. Running the same model configurations for both RCP and SSP scenarios, we see that the SSPs exhibit higher effective radiative forcing throughout the second half of the 21st Century. Comparing our results to the difference between CMIP5 and CMIP6 output, we find that the change in scenario explains approximately 46% of the increase in higher end projected warming between CMIP5 and CMIP6. This suggests that changes in ESMs from CMIP5 to CMIP6

https://doi.org/10.5194/gmd-2019-375
Preprint. Discussion started: 21 January 2020


Geoscientific Model Development Discussions

explain the rest of the increase, hence the higher climate sensitivities of available CMIP6 models may not be having as large an impact on GSAT projections as first anticipated. A second phase of RCMIP will complement RCMIP Phase 1 by exploring probabilistic results and emulation in more depth to provide results available for the IPCC's Sixth Assessment Report author teams.

Copyright statement. TEXT

1 Introduction

In an ideal world, sufficient computing power would enable running our most comprehensive, physically complete models for every application of interest. However, computational limits do exist so we must sometimes turn to other approaches. One common approach is the use of reduced complexity climate models (RCMs).

RCMs typically exchange limited spatial and temporal resolution for computational efficiency. Specifically, they usually focus on global-mean, annual-mean quantities. As a result, they are usually on the order of a million times faster than more complex models (in terms of simulated model years per unit CPU time).

The computational efficiency of RCMs means that they can be used where computational constraints would otherwise be limiting. Such cases include performing climate assessment for a large number of scenarios, exploring interacting uncertainties from multiple parts of the climate system or combining multiple lines of evidence in an internally consistent setup. In the IPCC context, a prominent example is the climate assessment of the WGIII socioeconomic scenarios. Given there are hundreds of emission scenarios submitted by Integrated Assessment Models in IPCC AR5 and AR6 (available at https://secure.iiasa.ac.at/web-apps/ene/AR5DB and https://tntcat.iiasa.ac.at/SspDb, hosted by the IIASA Energy Program) it is unfeasible to perform climate assessment with the world's most comprehensive models. Instead, reduced complexity models are used.

Beyond their computational efficiency, RCMs also offer conceptual simplicity. This gives them a second use: aiding in interpreting results from higher complexity models or observations. While we think this second use is also valuable (see e.g. Held et al. (2010) and Gregory (2004)), it is beyond the scope of this paper.

When RCMs are used to overcome computational constraints, they are typically used in one of two ways. 'Emulation' mode, where the RCMs are run in a setup which has been tuned to reproduce the behaviour of a Coupled Model Intercomparison Project (CMIP) (Eyring et al., 2016; Taylor et al., 2012) model as closely as possible over a range of scenarios. 'Probabilistic' mode, where the RCMs are run with a parameter ensemble which captures the uncertainty in historical observations. The resulting projections provide a plausible, observationally consistent range of projections which is large enough to provide useful statistics. In some cases they are also used in a combination of the two. For example, the MAGICC6 probabilistic setup used in the IPCC's Fifth Assessment Report (IPCC, 2013) used randomly drawn emulations for the carbon cycle response whilst using a probabilistic parameter ensemble for the climate response to radiative forcing (Meinshausen et al., 2009).

https://doi.org/10.5194/gmd-2019-375
Preprint. Discussion started: 21 January 2020


Geoscientific Model Development Discussions
Open Access
EGU

The validity of both approaches rests on the premise that RCMs are able to replicate the response characteristics of the Earth System and our most complete models. This ability is generally quantified in two different ways. The first is a comparison with observations. These comparisons provide the most direct comparison of model response with the world around us today. However, given the limited amount of observations available, comparing only with observations leaves us with little understanding of how RCMs perform in scenarios apart from one in which anthropogenic emissions are causing the climate to warm. Given our range of plausible futures, it is vital to also assess RCMs in other scenarios (e.g. reducing anthropogenic emissions, instantaneous changes in atmospheric CO2 concentrations, modifications to the solar constant). For example, an RCM that exhibits effectively constant climate feedbacks might be able to replicate an ESM's point response under an idealised scenario, but might not compare well to the longer-term response under either higher forcing or lower overshoot scenarios (Rohrschneider et al., 2019).

Whilst the results of more comprehensive models may not represent the behaviour of the actual earth system, they are the best representation of our knowledge of the earth system's behaviour. Comparing RCM behaviour with more complex model behaviour in these 'non-historical' experiments allows us to quantify the extent to which RCMs can capture the range of responses consistent with our best understanding of the earth system.

In Phase 1 of RCMIP we benchmark current RCM performance by comparing them with each other, observations and CMIP results over a range of experiments. This allows us to understand their strengths, weaknesses and limitations so that we can make more confident, informed conclusions from their quantitative results. RCMIP focuses on RCMs and is not one of the CMIP6 (Eyring et al., 2016) endorsed intercomparison projects that are designed for Earth System Models. However, RCMIP replicates the experimental design of many of the CMIP-endorsed MIPs, particularly the DECK simulations (Eyring et al., 2016), ScenarioMIP (O'Neill et al., 2016), AerChemMIP (Collins et al., 2017) and others, e.g. ZECMIP (Jones et al., 2019), DAMIP (Gillett et al., 2016) or PMIP4 (Kageyama et al., 2018).

RCMIP builds on previous efforts to compare and understand RCMs. In 1997, the IPCC Technical Paper (Houghton et al., 1997) investigated simple climate models used in the IPCC Second Assessment Report and compared their performance against idealised AOGCM results. Van Vuuren et al. (2011) compared RCMs used in integrated assessment models (IAMs). They focussed on five CO_2-only experiments to quantify the differences in the behaviour of each IAM's climate component (each of which is an RCM due to computational constraints). Harmsen et al. (2015) extended the work of van Vuuren et al. (2011) to consider the impact of non-CO_2 climate drivers in the RCPs. Recently, Schwarber et al. (2019) proposed a series of impulse tests for simple climate models in order to isolate differences in model behaviour under idealised conditions. RCMIP expands on the scope of previous work to include a broader range of scenarios and to make the first systematic comparison with both observations and CMIP model output.

1.1 Science questions

Over the course of its lifetime, RCMIP intends to answer the following scientific questions. This Phase 1 paper sets out the protocols required to do so. However, given the scope of the questions, they cannot all be answered in a single paper and so some aspects will receive less attention here than others.

https://doi.org/10.5194/gmd-2019-375
Preprint. Discussion started: 21 January 2020


Geoscientific Model Development Discussions

1. How do existing RCMs vary in their response to changes in well-mixed greenhouse gas (WMGHG) emissions, WMGHG concentrations, anthropogenic aerosol precursor emissions and natural changes in effective radiative forcing?
2. To what extent can RCMs emulate the response of more complex models from CMIP5 and CMIP6?
3. How do probabilistic ensembles from RCMs compare to each other and observations and what can they tell us about projected warming uncertainty under different scenarios?

2 Methods

2.1 Experimental design

Phase 1 of RCMIP focuses on a limited set of the CMIP6 experiment protocol plus a few experiments from CMIP5. On top of the experiments from CMIP6 and CMIP5 we also add other experiments which are of interest to the community (a full list is available in Supplementary Table S3). The first class of these are the 'esm-X-allGHG' experiments. These runs are driven by emissions of all greenhouse gases (CO_2, CH_4, HFCs, PFCs etc.), rather than only CO_2 as is typical for ESMs in CMIP6. These experiments are particularly useful to the WGIII community as they perform climate assessment based on emissions scenarios, hence need models which can run from emissions and do not require exogenous concentrations of greenhouse gases.

We also add one extra experiment, ssp370-lowNTCF-gidden, onto the ssp370-lowNTCF experiment from AerChemMIP. The ssp370-lowNTCF experiment explicitly excludes a reduction in methane concentrations. However, the ssp370-lowNTCF emissions dataset as described in Gidden et al. (2019) and calculated in Meinshausen et al. (2019) does include reduced methane emissions and hence atmospheric concentrations. We include a 'ssp370-lowNTCF-gidden' scenario to complement ssp370-lowNTCF and examine the consequences of a strong reduction in methane emissions.

The standard set of inputs from CMIP5 and CMIP6 was translated into the RCMIP experiment protocol, using the WGIII format (Gidden and Huppmann, 2019), so it could be used by the modelling groups.

CMIP6 emissions projections follow Gidden et al. (2019) and are taken from https://tntcat.iiasa.ac.at/SspDb/dsd?Action=htmlpage&page=60, hosted by IIASA. Where WMGHG gas emissions are missing, we use inverse emissions based on the CMIP6 concentrations from MAGICC7.0.0 (Meinshausen et al., 2019). Where regional emissions information is missing, we use the downscaling procedure described in Meinshausen et al. (2019). The emissions extensions also follow the convention described in Meinshausen et al. (2019).

For CMIP6 historical emissions, we have used data sources which match the harmonisation used for the CMIP6 emissions projections. This ensures consistency with CMIP6, albeit at the expense of using the latest data sources in some cases. CMIP6 historical anthropogenic emissions for CO_2, CH_4, BC, CO, NH_3, NOx, OC, SO_2 and volatile organic compounds (VOCs) come from CEDS (Hoesly et al., 2018). Biomass burning emissions data for CH_4, BC, CO, NH_3, NOx, OC, SO_2 and volatile organic compounds (VOCs) come from UVA (van Marle et al., 2017). The biomass burning emissions are a blend of both anthropogenic and natural emissions, which could lead to some inconsistency between RCMs as they make different assumptions about the particular anthropogenic/natural emissions split. CO_2 global land-use emissions are taken from the Global

https://doi.org/10.5194/gmd-2019-375
Preprint. Discussion started: 21 January 2020


Geoscientific Model Development Discussions

Carbon Budget 2016 (Quéré et al., 2016). Other CMIP6 historical emissions come from PRIMAP-hist (Gütschow et al., 2016) Version 1.0 https://doi.org/10.5880/PIK.2016.003 (N_2O and CO_2 land-use regional information). Where required, historical emissions were extended back to 1750 by assuming a constant relative rate of decline based on the period 1850-1860. While this means that our historical emissions are highly uncertain, all we require is consistent emissions inputs so we leave improved quantifications of emissions in this period for other research.

CMIP6 concentrations follow Meinshausen et al. (2019). CMIP6 radiative forcings follow the data provided at https://doi.org/10.5281/zenodo.3515339). CMIP5 emissions, concentrations and radiative forcings follow Meinshausen et al. (2011b) and are taken from http://www.pik-potsdam.de/~mmalte/rcps/.

2.2 Diagnostics

Given their focus on global-mean, annual mean variables we request a range of output variables from each RCM (detailed in Supplementary Table S4). The output variables focus on the response of the climate system to radiative forcing (e.g. surface air temperature change, surface ocean temperature change, effective radiative forcing, effective climate sensitivity) as well as the carbon cycle (carbon pool sizes, fluxes between the pools, fluxes due to Earth System feedbacks). The temporal resolution of the models means that we request the data on an annual timestep but may increase the temporal resolution in Phase 2.

The output dataset represents a huge data resource. In this paper we focus on a limited set of variables, particularly related to the climate response to radiative forcing. The dataset extends well beyond this limited scope and should be investigated in further research. To facilitate such research, we have put the entire database under a Creative Commons Attribution-ShareAlike 4.0 International (CC BY-SA 4.0) license.

2.3 Participating models

The models participating in RCMIP Phase 1 cover a broad spectrum of approaches (Table 1). In the climate response to radiative forcing, they range from two-box impulse response models to hemispherically resolved upwelling-diffusion ocean models and in the carbon cycle they range from no carbon cycle to regionally resolved, internal book-keeping modules. Technical details of the models are summarized in Supplementary Table S1 and described below.

2.3.1 ACC2

The Aggregated Carbon Cycle, Atmospheric Chemistry, and Climate model (ACC2) (Tanaka et al., 2007) is a reduced-complexity model developed from its predecessors (Hooss et al., 2001; Bruckner et al., 2003). ACC2 describes physical and biogeochemical processes of the earth system at the global-annual-mean level and comprises three modules: i) carbon cycle, ii) atmospheric chemistry and radiative forcing, and iii) climate. The carbon cycle module is a four-box atmosphere-ocean mixed layer model coupled with a four-box land biosphere model. Each box is characterized by a distinct time constant, capturing carbon cycle processes operating on different time scales. Saturating ocean CO_2 uptake under rising atmospheric CO_2 concentration is dynamically modeled by considering the thermodynamic equilibrium for ocean carbonate species. The

https://doi.org/10.5194/gmd-2019-375
Preprint. Discussion started: 21 January 2020


Geoscientific Model Development Discussions

CO_2 fertilization effect of the land biosphere is parameterized by the beta factor and assumed to depend logarithmically on the fractional change in the atmospheric CO_2 concentration relative to preindustrial. Carbon cycle processes are assumed to be insensitive to the change in surface temperature. ACC2 deals with the radiative forcing of CO_2, CH_4, N_2O, O_3, SF_6, 29 species of halocarbons, three types of aerosols, and stratospheric H_2O. The lifetime of CH_4 is related to the OH concentration, which further depends on the CH_4 concentration and NOx, CO, and VOC emissions. The climate module is the Diffusion Ocean Energy Balance Climate Model (DOECLIM) (Kriegler, 2005; Tanaka et al., 2007), a land-ocean energy balance model coupled with a heat diffusion model describing the heat transfer to the deep ocean.

Uncertain parameters such as climate sensitivity and beta factor for CO_2 fertilization are optimized based on an inverse estimation method considering historical observations and associated uncertainties (Tanaka et al., 2009). The model is thus designed to produce a set of 'best' outcomes under different assumptions, but not probabilistic outcomes. In RCMIP, model version 4.2 (Tanaka and O'Neill, 2018) is used.

2.3.2 AR5IR

The Fifth Assessment Report Impulse Response Model (AR5IR) was used for metric calculations in Chapter 8 of the IPCC's Fifth Assessment Report (Myhre et al., 2013b). Here we focus only on its temperature response to (effective) radiative forcing and do not incorporate any gas cycles. AR5IR is an impulse response model with two timescales by default. We also provide a three timescale version for comparison.

AR5IR is provided in a default setup which broadly reproduces historical GSAT observations with an equilibrium climate sensitivity of $3°C$. AR5IR has also been calibrated to the idealised CO_2-only experiments (abrupt-2xCO2, abrupt-4xCO2, abrupt-0p5xCO2, 1pctCO2) of a number of CMIP6 models. Only these calibrations are reported as emulating CMIP6 models for experiments including non-CO_2 climate drivers requires model specific estimates of non-CO_2 radiative forcings, which were not available during the calibration process. Throughout the calibrations, a default forcing due to a doubling of atmospheric CO_2 of 3.74 Wm^{-2} was chosen for simplicity. Using CMIP6 model specific values would not change results as it would simply cause all the calibrated parameters to be rescaled by a constant factor.

2.3.3 CICERO-SCM

The CICERO Simple climate model (CICERO-SCM) consists of an energy balance/upwelling diffusion model, a carbon cycle model (Joos et al., 1996) and simplified expressions relating emissions of 38 components to forcing, either directly or via concentrations (Skeie et al., 2017). The energy balance/upwelling diffusion model (Schlesinger et al., 1992) calculates warming separately for the two hemispheres and includes 40 vertical layers in the ocean. Heat is transported in the ocean by down welling of polar water and by diffusion. A posteriori distribution of the key parameters describing the mixing processes as well as the climate sensitivity and aerosol forcing has been estimated using observations of atmospheric temperature change and ocean heat content (Skeie et al., 2018).

The default model version used in this study has a climate sensitivity of $2.0°C$ and the rest of the parameters and the aerosol forcing is set to the mean value of the ensemble members with climate sensitivity in the range of 1.95 to $2.05°C$ from Skeie

https://doi.org/10.5194/gmd-2019-375
Preprint. Discussion started: 21 January 2020


Geoscientific Model Development Discussions

et al. (2018). For the model version with 3.0°C, the same approach is done for climate sensitivity in the range of 2.9 to 3.1°C. A detailed description of the CICERO-SCM is presented by Skeie et al. (2017). Here, new expressions of CO_2, CH_4 and N_2O radiative forcing (Etminan et al., 2016) are implemented in the SCM and indirect aerosol forcing is linearly scaled with SO_2 emissions rather than logarithmic as previously specified in the model. For the emission driven simulations, the time development of the natural emissions of N_2O and CH_4 are adjusted to match the observed historical concentration. The mean value of the natural emissions for the last 10 years is used for the future period.

2.3.4 ESCIMO

The Earth System Climate Interpretable Model (ESCIMO, Randers et al., 2016) is a system dynamics simulation model designed to make it simple and inexpensive for policy makers to estimate the effects of various possible human interventions proposed to influence the global mean temperature in this century. It is simple enough to run on a laptop in seconds, and to make it possible to understand what goes on in the model system. ESCIMO is one integrated model consisting of sectors that track i) global carbon flows, ii) global energy flows, and iii) global albedo change. ESCIMO, although simple, is capable of recreating the broad outline of the global climate history from 1850 to 2015. ESCIMO is also able to recreate the projections of global mean temperature GMST and other variables such as ice cover, ocean acidification, heat flow to the deep ocean, and carbon uptake in biomass, which are generated by the more complex climate models over the commonly used RCP scenarios. One feature of ESCIMO is that it generates run-away warming if global-mean land-ocean blended surface temperature (GMST) is allowed to rise more than 1°C relative to preindustrial times. However, the ensuing warming is slow and takes hundreds of years to lift the GMST by 3°C.

2.3.5 FaIR

The Finite-amplitude Impulse Response (FaIR) model is an emissions-driven simple climate model written in Python. FaIR v1.0 was originally designed to model the state-dependent carbon cycle with accumulated atmospheric carbon and temperature to CO_2 experiments (Millar et al., 2017) based on the impulse response relationship in IPCC AR5 (Myhre et al., 2013b), which is in turn built upon pulse-response experiments from Earth system models of full and intermediate complexity (Joos et al., 2013). The radiative forcing is coupled with a two time-constant global mean temperature response (Geoffroy et al., 2013). FaIR was extended to include emissions of non-CO_2 greenhouse gases and short-lived climate forcers in v1.3 (Smith et al., 2018a), reporting 13 categories of (effective) radiative forcing using simple emissions to forcing relationships available from AR5 and later (Etminan et al., 2016; Stevens, 2015; Ghan et al., 2013; Myhre et al., 2013b, a; Stevenson et al., 2013). FaIR v1.5 used in this analysis includes modules for inverting CO_2 concentrations to emissions and additional functionality required to run many of the experiments in RCMIP.

For the default case, a representative TCR of 1.7°C was chosen. Owing to tropospheric rapid adjustments (Smith et al., 2018b), an effective radiative forcing from a doubling of CO_2 of 4.01 Wm^{-2} is used, higher than the 3.71 Wm^{-2} used in (Myhre et al., 2013b). Furthermore, all experiments in this paper were run using the older GHG concentrations to radiative forcing relationships from Myhre et al. (2013b), firstly as the Etminan et al. (2016) relationship breaks down above 3000

https://doi.org/10.5194/gmd-2019-375
Preprint. Discussion started: 21 January 2020


Geoscientific Model Development Discussions

ppm CO2, and secondly because it is complicated to invert concentrations of CO_2 to emissions where CO_2 overlaps with other species in the radiative transfer parameterisation. To account for the substantial revision of methane radiative forcing in Etminan et al. (2016), the Myhre et al. (2013b) values are increased by 25%. For the probabilistic ensemble, a 300-member sample of ECS, TCR, carbon cycle sensitivity, effective radiative forcing (for non-aerosol forcing categories) and emissions to forcing parameters for aerosols were used, with the ensemble constrained based on 1850-2015 warming from reconstructed GSAT (Richardson et al., 2016).

2.3.6 GIR

GIR is a General Impulse Response Model built with the aim of achieving maximal simplicity, transparency and useability while remaining physically accurate enough for use in climate policy, research and teaching. It is based on the carbon cycle of FaIR v1.0 (Millar et al., 2017), but replaces a key model step – the numerical solution of a non-linear equation – with an analytic formula. It then extends the carbon cycle model out to other gases through parameter selection. The thermal response model is identical to the thermal response of both FaIR v1.0 and v1.5; though we allow the user to specify the number of thermal response timescales, rather than constraining the model to the usual two boxes. The model is therefore 6 equations in its entirety. The identical treatment of all greenhouse gases and aerosols (we find that aerosols can also be adequately represented through appropriate parameter selection) allows the model to take advantage of Python's array calculation infrastructure. It is therefore extremely rapid to run hundreds of thousands of scenario and parameter ensembles with GIR.

2.3.7 GREB

The Globally Resolved Energy Balance (GREB) model, also referred to as the Monash Simple Climate Model (MSCM) (Dommenget et al., 2019), is a 3.75°x 3.75°global model on three vertical layers: surface, atmosphere and subsurface ocean. It was originally developed to simulate the globally resolved surface temperature response to a change in CO_2 forcing, but is also used to study other elements of the mean climate state. The main physical processes that control the surface temperature tendencies are simulated: solar (short-wave) and thermal (long-wave) radiation, the hydrological cycle (including evaporation, moisture transport and precipitation), horizontal transport of heat and heat uptake in the subsurface ocean. Atmospheric circulation and cloud cover are a seasonally prescribed boundary condition, and state-independent flux corrections are used to keep the GREB model close to the observed mean climate. Thus, GREB does not simulate the atmospheric or ocean circulation and is therefore conceptually very different from GCM simulations.

The model does simulate important climate feedbacks such as water vapour and ice-albedo feedback, but an important limitation of the GREB model is that the response to external forcings does not involve circulation or cloud feedbacks (Dommenget and Flöter, 2011). The latest version (GREB v1.0.1) includes a new hydrological cycle model, which represents a simple and fast tool for the study of precipitation from a large-scale climate perspective, as well as to assess its response to climate variability (e.g. El Niño or climate change) and to external forcings. Three separate parameterisations are improved in the model: precipitation, evaporation and the circulation of water vapour (Stassen et al., 2019). A series of GREB experiment results and more introduction can be simply accessed on the official model website at http:

https://doi.org/10.5194/gmd-2019-375
Preprint. Discussion started: 21 January 2020


Geoscientific Model Development Discussions

//monash.edu/research/simple-climate-model/mscm/overview_i18n.html?locale=EN. The last stable version code is available on GitHub at https://github.com/christianstassen/greb-official/releases. For RCMIP scenarios, the model is run with all processes on. The climatology used for flux correction is taken from ERA-Interim Reanalysis IFS model (ECMWF_IFS) within a time window from 1979 to 2015. Other parameters and input variables (not initial conditions), are taken from either ERA-Interim or NCEP Reanalysis data.

2.3.8 Hector

Hector is an open-source, object-oriented, reduced-form global climate carbon-cycle model that includes simplified but physically-based representations of the most critical global-scale Earth system processes (Hartin et al., 2015; Vega-Westhoff et al., 2019). At each annual time step, Hector calculates a global change in radiative forcing from changes in atmospheric composition, and then passes this forcing to its climate core. The carbon cycle consists of three parts: a one-pool atmosphere, three-pool land, and four-pool ocean. The three terrestrial carbon cycle pools — vegetation, detritus, and soil — exchange carbon with the atmosphere through primary production (which increases with atmospheric CO_2 concentration) and heterotrophic respiration (which increases with temperature). Hector actively solves the inorganic carbon system in the surface ocean, directly calculating air-sea fluxes of carbon and ocean pH. A basic representation of thermohaline circulation drives heat and carbon exchange between low- and high-latitude surface ocean pools, an intermediate ocean pool, and a deep ocean pool. Besides CO_2, Hector also includes a basic representation of the atmospheric chemistry of halocarbons, O_3, NOx, and CH_4. The climate core of Hector is based on DOECLIM (Kriegler, 2005; Tanaka et al., 2007) and involves an analytical solution to ordinary differential equations governing heat exchange between the atmosphere and land, as well as a one-dimensional ocean heat diffusion model. Hector is written in C++ and can be run as a standalone executable, coupled to an integrated assessment model, as well as via a Python (Willner et al., 2017) or R package. Hector's flexibility, open-source nature, and modular design facilitates a broad range of research in various areas.

Four Hector climate parameters, S, κ (ocean heat diffusivity), α_a (aerosol forcing scaling factor), and α_v (volcanic forcing scaling factor) were calibrated to six individual CMIP6 ESMs. The calibration protocol implemented followed Dorheim et al. (Under Review at Earth and Space Science) that utilises concentration-driven historical temperature and future multi-forcing scenario temperature and ocean heat flux as comparison data in a nonlinear optimization calibration. For the 'probabilistic' Hector simulations in this study, we used 1000 random draws from joint posterior parameter distributions from the Bayesian calibration of Hector against historical observations in Vega-Westhoff et al. (2019).

2.3.9 Held et al. two layer model

The Held et al. two layer model (University of Melbourne implementation) is based on Held et al. (2010) with a state-dependent feedback factor following Rohrschneider et al. (2019). It uses a two-layer ocean model to simulate the temperature response to (effective) radiative forcing.

The Held two layer model is provided in a default setup which broadly reproduces historical GSAT observations with an equilibrium climate sensitivity of 3°C. It has also been calibrated to the idealised CO_2-only experiments (abrupt-2xCO2,

https://doi.org/10.5194/gmd-2019-375
Preprint. Discussion started: 21 January 2020


Geoscientific Model Development Discussions
Open Access
EGU

abrupt-4xCO2, abrupt-0p5xCO2, 1pctCO2) of a number of CMIP6 models. Only these calibrations are reported as emulating CMIP6 models for experiments including non-CO_2 climate drivers requires model specific estimates of non-CO_2 radiative forcings, which were not available during the calibration process. Throughout the calibrations, a default forcing due to a doubling of atmospheric CO_2 of 3.74 Wm^{-2} was chosen for simplicity. Using CMIP6 model specific values would marginally improve the fits and the correspondence between fitted parameters and ESM properties.

2.3.10 MAGICC

MAGICC, the 'Model for the Assessment of Greenhouse Gas Induced Climate Change' has its origins in early upwelling-diffusion ocean parameterisations by Wigley and Schlesinger (1985), with components for sea level rise (Wigley and Raper, 1987) and a carbon cycle being added subsequently (Wigley, 1991). MAGICC has been used frequently in all past IPCC reports, often in conjunction with the ISAM (Jain et al., 1994) and Bern-CC (Siegenthaler and Joos, 1992) carbon cycle models. Initially, MAGICC was written in Fortran 77, then transferred to Fortran 90 in the 2000s (Meinshausen et al., 2011a, c), amended by a permafrost module (von Deimling et al., 2012) and a new sea level rise module (Nauels et al., 2017). An updated version (MAGICC7.0.0) was used to generate the GHG concentration projections that are the input assumptions for the CMIP6 ESM experiments (Meinshausen et al., 2019), mainly in ScenarioMIP, but also in AerChemMIP and PMIP4. MAGICC7.0.0 also included several updated radiative forcing parameterisations, including a CO_2, CH_4 and N_2O parameterisation that capture results by Etminan et al. (2016), while allowing for a wider range of input concentrations (see Meinshausen et al. (2019) for details).

For the calibration to individual CMIP6 models, three key advances have been made since MAGICC7.0.0. Firstly, a land heat capacity term was included. Previously, only the ocean provided heat capacity in the energy balance model with ocean heat uptake equalling the parameterised radiative flux imbalance at the top of the atmosphere. Secondly, the parameterisation of the sensitivity of climate sensitivity to the overall forcing magnitude has been adapted. Previously, this sensitivity was implemented as an independent scaling of land and ocean feedback parameters (Meinshausen et al., 2011a). In MAGICC7.1.0, there are two parameterisations that allow for a time-changing effective climate sensitivity - apart from the geometric effect that arises from constant land and ocean feedback parameters but time-changing ratios of land and ocean warming. The first is an option for the calibration routine to allow a linear adjustment of the climate sensitivity with a forcing change, pegged at doubled CO_2 concentration. This immediate adjustment of the climate sensitivity is independent from the second one, which allows for a slow and inert response, such as to parameterise the slow change of albedo with melting ice caps. This second sensitivity adjustment is assumed to be proportional to the cumulative temperature over a window of several hundred years. Given the wide range of different experiments in the CMIP6 archives, ranging from highly idealized scenarios to multi-gas 21st century results, MAGICC's calibration routines (which calibrate to all available scenarios, both idealised, and multi-gas scenarios at once) can differentiate between immediate and inert climate sensitivity adjustment terms.

https://doi.org/10.5194/gmd-2019-375
Preprint. Discussion started: 21 January 2020


Geoscientific Model Development Discussions

2.3.11 MCE

MCE, a minimal CMIP emulator, is a tool for diagnosing and emulating the global behavior of complex AOGCMs with minimally required parameters for both simplicity and accuracy. It consists of a thermal response module and a carbon cycle module. The thermal response, described in Tsutsui (2017), is represented by the sum of three exponentials as an impulse response function to effective radiative forcing, assuming a constant climate feedback parameter. The forcing model uses logarithmic scaling in terms of atmospheric CO_2 concentrations and its amplification from the first to the second doubling. Non-CO_2 forcing is not explicitly considered. The carbon cycle is based on Hooss et al. (2001) and Joos et al. (1996) and additionally incorporates simple climate-carbon cycle feedback for the chemical equilibrium of the marine inorganic carbon cycle and the decay of organic materials in the terrestrial biosphere.

The thermal response and forcing parameters are calibrated to temperature and heat uptake timeseries from abrupt-4xCO2 and 1pctCO2 experiments of a target AOGCM, from which ECS and TCR are diagnosed (Tsutsui, Submitted to Geophysical Research Letters). The diagnosed ECS is properly scaled down from an estimated equilibrium temperature increase to a quadrupling forcing level. The current calibration includes individual model emulation for 25 CMIP5 models and 22 CMIP6 models, and five representative sets adjusted to nominal quantiles of 0.17, 0.33, 0.5, 0.67, and 0.83 in terms of transient climate response to cumulative CO_2 emissions (TCRE) based on the likely range assessed in the IPCC Fifth Assessment Report (Collins et al., 2013). The carbon cycle parameters are crudely calibrated to historical carbon balance assessed in AR5 (Ciais et al., 2013), and mean properties of CMIP5 ESMs (Arora et al., 2013), and are fixed across all model configurations. The TCRE-based median calibration is close to the current default configuration, which is defined as a CMIP5 mean.

2.3.12 OSCAR

OSCAR v3.0 is an open-source reduced-form Earth system model, whose modules mimic models of higher complexity in a probabilistic setup (Gasser et al., 2017a). The response of the global surface temperature to radiative forcing follows a two-box model formulation (Geoffroy et al., 2013). OSCAR calculates the radiative forcing caused by greenhouse gases (CO_2, CH_4, N_2O, 37 halogenated compounds), short-lived climate forcers (tropospheric and stratospheric ozone, stratospheric water vapor, nitrates, sulfates, black carbon, primary and secondary organic aerosols) and changes in surface albedo. The ocean carbon cycle is based on the mixed-layer response function of Joos et al. (1996), albeit with an added stratification of the upper ocean derived from CMIP5 (Arora et al., 2013) and with an updated carbonate chemistry. The land carbon cycle is divided into five biomes and five regions, and each of the 25 biome/region combinations follows a three-box model (soil, litter and vegetation). The pre-industrial state of the land carbon cycle is calibrated to TRENDYv2 (Sitch et al., 2015) and its transient response to CO_2 and climate is calibrated to CMIP5 (Arora et al., 2013). Land cover change, wood harvest and shifting cultivation are also accounted for, thanks to a dedicated book-keeping module that allows OSCAR to estimate its own CO_2 emissions from land-use change (Gasser et al., 2017b). Permafrost thaw and the consequent emission of CO_2 and CH_4 is also modeled (Gasser et al., 2018). CH_4 emissions from wetlands are calibrated on WETCHIMP (Melton et al., 2013). In addition, biomass burning emissions are calculated endogenously following the book-keeping module and the wildfire feedback. These emissions were therefore

https://doi.org/10.5194/gmd-2019-375
Preprint. Discussion started: 21 January 2020


Geoscientific Model Development Discussions

subtracted from the input RCMIP data used to drive OSCAR to avoid double counting. The atmospheric lifetimes of non-CO_2 greenhouse gases are impacted by non-linear tropospheric (Holmes et al., 2013) and stratospheric (Prather et al., 2015) chemistry. Tropospheric ozone follows the formulation by Ehhalt et al. (2001) but recalibrated to ACCMIP (Stevenson et al., 2013). Stratospheric ozone is derived from Newman et al. (2006) and Ravishankara et al. (2009). Aerosol-radiation interactions are based on CMIP5 and AeroCom2 (Myhre et al., 2013a), and aerosol-cloud interactions depend on the hydrophilic fraction of each aerosol and follow a logarithmic formulation (Hansen, 2005). Surface albedo change induced by land-cover change follows Bright and Kvalevåg (2013). The one induced by deposition of black carbon on snow is calibrated on ACCMIP globally (Lee et al., 2013) and then regionalized (Reddy and Boucher, 2007).

In this project, 10000 elements of a Monte-Carlo ensemble were generated, and each simulation was run using all these configurations. Each configuration was then weighted by comparing its results in the concentration-driven historical simulation to observations. Four observations were used: (i) the increase in global surface temperature from 1850-1900 to 2006-2015 (Allen et al., 2018), (ii) the cumulative ocean heat sink over 1959-2017, (iii) the cumulative fossil-fuel CO_2 emissions over 1959-2017, and (iv) the average fossil-fuel CO_2 emissions over 2000-2009 (Quéré et al., 2018). All final outputs are provided as the resulting weighted means and standard deviations. This constraining setup leads to an equilibrium climate sensitivity of 2.65 ± 0.46 °C. We did not further constrain our ensemble.

2.3.13 WASP

The Warming Acidification and Sea level Projector (WASP) is an efficient Earth system model capable of producing a large ensemble of simulations on a standard desktop computer. WASP comprises an 8-box representation of the coupled atmosphere-ocean-land system (Goodwin, 2016). The atmosphere comprises a single box connected to the land and ocean systems. The land system comprises a vegetation carbon box with CO_2 and temperature dependent net primary production, and a soil carbon box with temperature dependent carbon respiration. The ocean comprises a surface mixed layer box, exchanging heat and carbon with 4 sub-surface boxes (Goodwin, 2016). The exchange of carbon dioxide between the atmosphere and surface ocean boxes is solved via a buffered carbon inventory approach (Goodwin et al., 2014), avoiding the computational expense of iteratively solving seawater carbonate chemistry. Global mean surface warming is solved via the extended energy balance equation of (Goodwin et al., 2014). The version of WASP used here adopts time-evolving climate feedbacks as described in Goodwin (2018), with separate climate feedback terms representing processes such as cloud feedback, water vapour-lapse rate feedback and surface albedo feedback. The WASP model is coded in C++, with the code for the version used here available from the supplementary material of Goodwin (2018).

Initially, a 10 million member ensemble is generated with the values of 21 input parameters varied independently between simulations. The 21 input parameter distributions are as described in Goodwin (2018), except that here: (i) the surface ocean carbon uptake e-folding timescale is varied from a uniform random distribution between the limits of 0.5 years and 1.0 years, and (ii) the sensitivity of soil carbon residence timescale to temperature is varied from a random-normal distribution with mean -1.36 yr K^{-1} and standard deviation 0.45 yr K^{-1}, to match the variation seen in Dynamic Global Vegetation Models used in Pugh et al. (2018). Each simulation is integrated from years 1765 to 2018 using historical forcing. All 10 million

https://doi.org/10.5194/gmd-2019-375
Preprint. Discussion started: 21 January 2020


Geoscientific Model Development Discussions

initial ensemble members are then assessed against an observational consistency test (Goodwin, 2018) using the methodology described in Goodwin et al. (2018). The observational consistency test comprises assessment of global surface warming, sea surface temperature warming, ocean heat uptake, ocean carbon uptake and land carbon uptake over various historical periods, resulting in observation consistent constraints on the ranges of physical climate feedbacks Goodwin (2018) and land carbon feedbacks (Goodwin et al., 2019). Around 2000 simulations pass the observational consistency test and are accepted into the final observation-constrained model ensemble. This final model ensemble thus contains the small number of parameter value combinations that produce observation-consistent simulations, in which the values of the 21 input parameters are no longer independent of one another. The observation-constrained simulations are integrated into the future for the SSP scenarios (using non-CO_2 radiative forcing following the Effective Radiative Forcing from Shared Socioeconomic Pathways available at https://doi.org/10.5281/zenodo.3515339). To perform the idealised scenarios, that do not have a historically forced period with which to extract the final ensemble, the final observation-consistent model ensemble generated from the ssp585 scenario is used. Due to the observational constraints used for surface warming, the WASP model's primary global surface temperature anomaly variable represents a blended land and ocean temperature (GMST). To calculate surface air temperature (GSAT) for the RCMIP results, the GMST is divided by 0.95 (Cowtan et al., 2015).

3 Results and Discussion

RCMs agree moderately well with historical observations of global-mean surface air temperature (GSAT) (Figure 1). For the period 2000-2019, the RCMs project warming of 0.94°C with a standard deviation of 0.09°C relative to a reference period of 1850-1900 and a warming rate of 0.24°C / decade with a standard deviation of 0.04°C / decade. These projections agree with best-guess warming observations of 0.99°C but no RCM agrees with the observed warming rate of 0.19°C / decade. With the exception of the GREB model (which is a CO_2-only model), all the RCMs demonstrate an ability to reproduce short-term cooling due to major volcanic eruptions.

The RCMs do not exhibit the same high-frequency modes as observations due to their lack of internal variability, particularly representations of phenomena like El Nino, the Interdecadal Pacific Oscillation or Atlantic Meridional Variability. This lack of natural variability may explain why RCMs (with the exception of GREB which is a CO_2-only model) appear to be too cool through the 1960's, 70's and 80's and then warm too quickly thereafter. Alternately, it could be that RCMs overestimate aerosol cooling over this period (although the spread in aerosol effective radiative forcing estimates across models is nonetheless fairly large, see Supplementary Figure S1) or overestimate of the impact of the eruption of Mt Agung in 1963.

This suggests a clear area for further evaluation of RCMs and has important implications for remaining carbon budget estimates, which are highly sensitive to estimates of recent warming trends (Leach et al., 2018). Discrepancies in the carbon cycle response to emissions also impact remaining carbon budget estimates, and further analysis on the all-greenhouse gas emissions driven runs would highlight further model differences.

The discrepancies between RCMs are of a similar order of magnitude to observational uncertainties (Morice et al., 2012). The spread of RCMs is also much smaller than the spread in available CMIP6 model results (warming of 1.13 ± 0.3°C and

https://doi.org/10.5194/gmd-2019-375
Preprint. Discussion started: 21 January 2020


Geoscientific Model Development Discussions

warming rate of $0.24 \pm 0.08°C$ / decade when only the first available ensemble member from each model group is used). Given their simple, tuneable nature, it is no surprise that RCMs tend to agree more closely with observations than CMIP models and exhibit less spread.

In general, RCMs can emulate CMIP6 surface air temperature change relatively well (Figure 2). Given that RCMs do not include internal variability, the lower bound for root-mean square error (RMSE) is of the same order of magnitude as internal variability in CMIP6 models. The best emulators are pushing this limit, with RMSE on the order of 0.2K (Table 2). As CMIP6 results have only recently become available, we expect further calibration efforts to reduce RMSE even further.

Despite their relatively good performance, results for the different emulation setups have generally only been submitted for a limited set of scenarios (see Supplementary Table S2 and Supplementary Figures S7 - S33). Hence it is still not clear whether the good performance in idealised scenarios also carries over to projections, particularly for the SSPs. Having said this, results for MAGICC7.1.0, which has supplied projections for the SSPs for each emulation setup, are promising. MAGICC7.1.0's results suggest that RCMs should be close to the lower limit of RMSE as more CMIP6 results become available and further calibration efforts are carried out.

From the available results, differences emerge between models with constant effective climate sensitivities and models with time or state dependent effective climate sensitivities. Models with constant effective climate sensitivities, such as the AR5IR implementations, struggle to capture the non-linear response of ESMs to abrupt changes in CO_2 concentrations. Firstly, they predict an equally large response to negative radiative forcing as positive radiative forcing which isn't always the case in ESMs (Panels (d) and (e) of Figure 2). Secondly, in order to capture the long-term warming seen in many abrupt-4xCO2 experiments, one of the boxes often has a response timescale on the order of thousands of years. This is problematic because it leads to equilibration times on the order of thousands of years and large equilibrium responses in the abrupt-2xCO2 experiments (i.e. large equilibrium climate sensitivities, see Supplementary Table S2). Models with time or state dependent effective climate sensitivities avoid both those problems. In particular, their temperature response to positive and negative radiative forcing need not be of equal magnitude and they can exhibit the long warming tail seen in ESM abrupt-4xCO2 runs whilst avoiding extremely long equilibration times and large equilibrium temperature perturbations in abrupt-2xCO2 runs.

Probabilistic projections from RCMs illustrate the large range of plausible temperature projections resulting from physical parameter sets which are consistent with observations (Figure 3). For example, under the very ambitious mitigation scenario ssp119, the models presented here have a best estimate of approximately $1.5°C$ for end of century warming. However, they also suggest that there is still approximately a 1 in 6 chance that warming would exceed $2°C$.

These probabilistic projections extend the results of CMIP6, which do not include such large perturbed parameter ensemble plus constraining exercises. The 66% ranges presented here are, in general, significantly narrower than the CMIP6 intermodel spread. There is no requirement that CMIP6 results lie within some range of historically observed temperature changes but the difference suggests that some caution should be used when inferring projection uncertainty from CMIP6 results alone.

Four of the models (MCE, WASP, FaIR and OSCAR) provide remarkably similar median projections. On the other hand, Hector projects significantly smaller surface air temperature increases, likely due to its lower CO_2 radiative forcing estimates (Figure S2).

https://doi.org/10.5194/gmd-2019-375
Preprint. Discussion started: 21 January 2020


Geoscientific Model Development Discussions

On the other hand, there is a surprising amount of variation in probabilistic simulations of the historical period. The variation in ranges, from MCE with relatively large ranges, to WASP and Hector with much smaller ranges, likely reflects differences in constraining techniques. Given that variations in both model structure and calibration technique influence probabilistic projections, an area for future research could be to try and disentangle the impact of these two components. Such an experiment could involve constraining models with the same constraining technique or constraining a single model with two different techniques.

One other area for future research is the impact of the reference period. Within the reference period, all model results and observations will be artificially brought together, narrowing uncertainty and disagreement within this period (Hawkins and Sutton, 2016). This can alter conclusions as the reference period will become less important for any fitting algorithm (because of the artificial agreement), placing more weight on other periods. Developing a method to rebase both the mean and variance of model and observational results onto other reference periods would allow the impact of the reference period choice to be explored in a more systematic fashion.

Looking forward, it is clear that making probabilistic projections consistent with CMIP6 results requires structural model flexibility, such that models are shown to be able to reproduce CMIP6 results. Having achieved this, probabilistic parameter ensembles can then be derived while considering uncertainty in both CO_2 and non-CO_2 climate drivers. During RCMIP Phase 1, only Hector has been able to perform both these steps. However, we hope that more models will be able to perform these steps in further phases. Such results would enhance our understanding of the uncertainty in observationally consistent climate change projections and hence be of interest to the climate research community and beyond.

When run with the same model, warming projections are higher in the SSPs than the RCPs (Figure 4). Whilst historical warming estimates are very similar, if not slightly higher in the RCP-compatible historical runs, the scenarios separate over the course of the 21st Century.

For the RCMIP results, we can see that the increase in warming projections is due to the higher effective radiative forcing in the SSPs throughout the second half of the 21st Century (Supplementary Figure S3). The higher effective radiative forcing results appears to be a result of the SSPs agreeing more closely with their nameplate 2100 radiative forcing level than the RCPs, which were generally too low. The increased forcing is driven largely by increased CO_2 effective radiative forcing (Supplementary Figure S4), which itself is driven by increased CO_2 emissions (Gidden et al., 2019). Even though aerosol effective radiative forcing is also slightly more negative in the SSPs (Supplementary Figure S5), the difference of approximately 0.1 Wm^{-2} is not enough to offset increased CO_2 effective radiative forcing of approximately 0.5 Wm^{-2}.

At present, effective radiative forcings diagnosed from the CMIP6 models are not available (as such diagnosis is not a trivial task). However, given the monotonic relationship between CO_2 concentrations and effective radiative forcing (Myhre et al., 2013b), it is likely that the same mechanisms are driving at least part of the increase between CMIP5 and CMIP6 projections.

Comparing warming projections between CMIP5 and CMIP6, our results suggest that around 46% of the increase is scenario driven. However, this still leaves 54% which is not explained by the change in scenarios. At this stage, this residual is most likely explained by a change in the models submitting results to CMIP, which appear to be more sensitive to changes in

https://doi.org/10.5194/gmd-2019-375
Preprint. Discussion started: 21 January 2020


Geoscientific Model Development Discussions

atmospheric GHG concentrations in CMIP6 than in CMIP5 (Wyser et al., 2019; Voldoire et al., 2019; Voosen, 2019). However, CMIP6 analysis is ongoing and should be considered before making strong conclusions about the robustness of these findings.

As discussed previously, the results from RCMIP can provide much more information than has been presented here. A number of experiments have not been discussed here which would shed light on the differences between the RCMs in a number of other components. In addition, RCMs also offer the chance to explore more experiments than is planned in CMIP6 due to their computational efficiency. An experiment which is an example of both these points is the ssp370-lowNTCF scenario as quantified by Gidden et al. (2019), which includes reductions in methane emissions. In contrast, the ssp370-lowNTCF as defined by AerChemMIP explicitly includes methane emissions reductions. RCMs can examine the impact of this difference by running an extra experiment, 'ssp370-lowNTCF-gidden', which follows the emissions quantified by Gidden et al. (2019). Preliminary results are given in Supplementary Figure S6 and, unsurprisingly, show that surface air temperatures rise in ssp370-lowNTCF (relative to ssp370) whilst they fall in ssp370-lowNTCF-gidden. This fall in temperatures is driven entirely by reductions in methane emissions and users of CMIP6 data should be careful not to confuse the results of the ssp370-lowNTCF scenario with the emissions scenarios presented in Gidden et al. (2019). They are two different experiments.

4 Conclusions

Phase 1 of RCMIP has identified some of the strengths, weaknesses and limitations of various RCMs which exist in the literature today. This paper has focussed on surface air temperature (GSAT) changes but many more output variables are available in the Phase 1 database. To facilitate further research, the entire database is available under a Creative Commons Attribution-ShareAlike 4.0 International (CC BY-SA 4.0) license.

We have found that RCMs are capable of reproducing broad-scale characteristics of observed historical GSAT changes as well as the response of ESMs under various experiments. Further work could focus on why RCMs exhibit relatively high recent warming rates compared to observations and using the ever growing body of CMIP6 results to improve RCM emulation capabilities. Nonetheless, there is clear evidence that the addition of time and state-dependent climate feedbacks in many RCMs has improved their ability to emulate the behaviour of more complex models under a range of forcing conditions.

Probabilistic projections from RCMs complement higher complexity model results by providing uncertainties which are by design consistent with historically observed temperature changes. Further evaluating these probabilistic distributions and the impact of different derivation techniques and model structures is a clear next step for the RCM community. Another next step is adding more models which are both calibrated to CMIP6 results and have probabilistic distributions as only the Hector model has managed this to date.

Phase 1 paves the way for further phases of RCMIP. Much of the work of defining community standards, data handling practices and communication methods has been established and now only needs refining. Further phases of RCMIP could focus on many different themes, for example, considering a wider range of variables, probabilistic climate projections (something which cannot be done with more complex models due to computational expense), specific components of the earth system (e.g.

https://doi.org/10.5194/gmd-2019-375
Preprint. Discussion started: 21 January 2020


Geoscientific Model Development Discussions

ocean heat content, representation of aerosols, sea-level rise) or model development (e.g. adding new components to models). We would welcome requests, suggestions and further involvement from throughout the climate modelling research community.

Code and data availability. RCMIP input timeseries and results data along with processing scripts as used in this submission are available from the RCMIP GitLab repository at https://gitlab.com/rcmip/rcmip and archived by Zenodo (https://doi.org/10.5281/zenodo.3593570).

The ACC2 model code is available upon request.

The implementation of the AR5IR model used in this study is available in the OpenSCM repository: https://github.com/openclimatedata/openscm/blob/ar5ir-notebooks/notebooks/ar5ir_rcmip.ipynb

The model version of ESCIMO used to produce the RCMIP runs can be downloaded from http://www.2052.info/wp-content/uploads/2019/12/mo191107%202%20ESCIMO-rcimpfrom%20mo160911%202100%20ESCIMO.vpm. The vpm extension allows you to view, examine and run the model, but not save it. The original model with full documentation is available from http://www.2052.info/escimo/.

FaIR is developed on GitHub at https://github.com/OMS-NetZero/FAIR and v1.5 used in this study is archived at Zenodo (Smith et al., 2019).

The GREB model source code used is available, upon request, on Bitbucket: https://bitbucket.org/rcmipgreb/greb-official/src/official-rcmip/. The last stable versions are available on GitHub at https://github.com/christianstassen/greb-official/releases.

The Held two layer model (uom implementation) is available in the OpenSCM repository: https://github.com/openclimatedata/openscm/blob/ar5ir-notebooks/notebooks/held_two_layer_rcmip.ipynb

Hector is developed on GitHub at https://github.com/JGCRI/hector. The exact version of Hector used for these simulations can be found at https://github.com/JGCRI/hector/releases/tag/rcmip-tier1. The scripts for the RCMIP runs are available at https://github.com/ashiklom/hector-rcmip.

MAGICC's Python wrapper is archived at Zenodo (https://doi.org/10.5281/zenodo.1111815) and developed on GitHub at https://github.com/openclimatedata/pymagicc/.

OSCAR v3 is available on GitHub at https://github.com/tgasser/OSCAR.

WASP's code for the version used in this study is available from the supplementary material of Goodwin Goodwin (2018): https://doi.org/10.1029/2018EF000889. See also the WASP website at http://www.waspclimatemodel.info/download-wasp.

The other participating models are not yet available publicly for download or as open source. Please also refer to their respective model description papers for notes and code availability.

Author contributions. ZN and RG conceived the idea for RCMIP. ZN, MM and JL setup the RCMIP website (rcmip.org), produced the first draft of the protocol and derived the data format. All authors contributed to updating and improving the protocol. ACC2 results were provided by KT and EK. AR5IR and Held et al. two layer model were provided by ZN. CICERO-SCM results were provided by JF, BS, MS and RS. ESCIMO results were provided by UG. FaIR results were provided by CS. GIR results were provided by NL. GREB results were provided by DD, CF, DM and ZX. Hector results were provided by AS and KD. MAGICC results were provided by MM, JL and ZN. MCE results were provided by JT. OSCAR results were provided by TG and YQ. WASP results were provided by PG. ZN wrote, except for the model descriptions, the first manuscript draft, produced all the figures and led the manuscript writing process with support from RG. All authors contributed to writing and revising the manuscript.

https://doi.org/10.5194/gmd-2019-375
Preprint. Discussion started: 21 January 2020


Geoscientific Model Development Discussions

Competing interests. The authors declare that they have no conflict of interest.

Acknowledgements. We acknowledge the World Climate Research Program (WCRP) Coupled Model Intercomparison Project (CMIP) and thank the climate modeling groups for producing and making available their model output. RCMIP could not go ahead without the outputs of CMIP6 nor without the huge effort which is put in by all the researchers involved in CMIP6 (some of whom are also involved in RCMIP).

We also thank the RCMIP Steering Committee, comprised of Jan Fuglestvedt, Maisa Corradi, Malte Meinshausen, Piers Forster, Joeri Rogelj and Steven Smith, for their support and guidance throught Phase 1. We look forward to their ongoing support in further phases.

ZN benefited from support provided by the ARC Centre of Excellence for Climate Extremes (CE170100023). KT is supported by the Integrated Research Program for Advancing Climate Models (TOUGOU Program), the Ministry of Education, Culture, Sports, Science, and Technology (MEXT), Japan.

https://doi.org/10.5194/gmd-2019-375
Preprint. Discussion started: 21 January 2020

References

Allen, M. R., Dube, P. D., Solecki, W., Aragón-Durand, F., Cramer, W., Humphreys, S., Kainuma, M., Kala, J., Mahowald, N., Mulugetta, Y., Perez, R., Wairiu, M., and Zickfeld, K.: Framing and Context, World Meteorological Organization, Geneva, Switzerland, https://www.ipcc.ch/sr15/, 2018.

Arora, V. K., Boer, G. J., Friedlingstein, P., Eby, M., Jones, C. D., Christian, J. R., Bonan, G., Bopp, L., Brovkin, V., Cadule, P., Hajima, T., Ilyina, T., Lindsay, K., Tjiputra, J. F., and Wu, T.: Carbon–Concentration and Carbon–Climate Feedbacks in CMIP5 Earth System Models, Journal of Climate, 26, 5289–5314, https://doi.org/10.1175/jcli-d-12-00494.1, 2013.

Bright, R. M. and Kvalevåg, M. M.: Technical Note: Evaluating a simple parameterization of radiative shortwave forcing from surface albedo change, Atmospheric Chemistry and Physics, 13, 11 169–11 174, https://doi.org/10.5194/acp-13-11169-2013, 2013.

Bruckner, T., Hooss, G., Füssel, H.-M., and Hasselmann, K.: Climate System Modeling in the Framework of the Tolerable Windows Approach: The ICLIPS Climate Model, Climatic Change, 56, 119–137, https://doi.org/10.1023/a:1021300924356, 2003.

Ciais, P., Sabine, C., Bala, G., Bopp, L., Brovkin, V., Canadell, J., Chhabra, A., DeFries, R., Galloway, J., Heimann, M., Jones, C., Le Quéré, C., Myneni, R., Piao, S., and Thornton, P.: Carbon and Other Biogeochemical Cycles, book section 6, p. 465–570, Cambridge University Press, Cambridge, United Kingdom and New York, NY, USA, https://doi.org/10.1017/CBO9781107415324.015, http://www.climatechange2013.org, 2013.

Collins, M., Knutti, R., Arblaster, J., Dufresne, J.-L., Fichefet, T., Friedlingstein, P., Gao, X., Gutowski, W., Johns, T., Krinner, G., Shongwe, M., Tebaldi, C., Weaver, A., and Wehner, M.: Long-term Climate Change: Projections, Commitments and Irreversibility, book section 12, p. 1029–1136, Cambridge University Press, Cambridge, United Kingdom and New York, NY, USA, https://doi.org/10.1017/CBO9781107415324.024, http://www.climatechange2013.org, 2013.

Collins, W. J., Lamarque, J.-F., Schulz, M., Boucher, O., Eyring, V., Hegglin, M. I., Maycock, A., Myhre, G., Prather, M., Shindell, D., and Smith, S. J.: AerChemMIP: quantifying the effects of chemistry and aerosols in CMIP6, Geoscientific Model Development, 10, 585–607, https://doi.org/10.5194/gmd-10-585-2017, 2017.

Cowtan, K., Hausfather, Z., Hawkins, E., Jacobs, P., Mann, M. E., Miller, S. K., Steinman, B. A., Stolpe, M. B., and Way, R. G.: Robust comparison of climate models with observations using blended land air and ocean sea surface temperatures, Geophysical Research Letters, 42, 6526–6534, https://doi.org/10.1002/2015gl064888, 2015.

Dommenget, D. and Flöter, J.: Conceptual understanding of climate change with a globally resolved energy balance model, Climate Dynamics, 37, 2143–2165, https://doi.org/10.1007/s00382-011-1026-0, 2011.

Dommenget, D., Nice, K., Bayr, T., Kasang, D., Stassen, C., and Rezny, M.: The Monash Simple Climate Model experiments (MSCM-DB v1.0): an interactive database of mean climate, climate change, and scenario simulations, Geoscientific Model Development, 12, 2155–2179, https://doi.org/10.5194/gmd-12-2155-2019, 2019.

Dorheim, K., Link, R., Hartin, C., Kravitz, B., and Snyder, A.: Calibrating simple climate models to individual Earth system models: Lessons learned from calibrating Hector, Under Review at Earth and Space Science.

Ehhalt, D., Prather, M., Dentener, F., Derwent, R., Dlugokencky, E., Holland, E., Isaksen, I., Katima, J., Kirchhoff, V., Matson, P., Midgley, P., and Wang, M.: Atmospheric Chemistry and Greenhouse Gases, https://www.ipcc.ch/site/assets/uploads/2018/03/TAR-04.pdf, 2001.

Etminan, M., Myhre, G., Highwood, E. J., and Shine, K. P.: Radiative forcing of carbon dioxide, methane, and nitrous oxide: A significant revision of the methane radiative forcing, Geophysical Research Letters, 43, 12,614–12,623, https://doi.org/10.1002/2016gl071930, 2016.

https://doi.org/10.5194/gmd-2019-375
Preprint. Discussion started: 21 January 2020

Eyring, V., Bony, S., Meehl, G. A., Senior, C. A., Stevens, B., Stouffer, R. J., and Taylor, K. E.: Overview of the Coupled Model Intercomparison Project Phase 6 (CMIP6) experimental design and organization, Geoscientific Model Development (Online), 9, 2016.

Gasser, T., Ciais, P., Boucher, O., Quilcaille, Y., Tortora, M., Bopp, L., and Hauglustaine, D.: The compact Earth system model OSCAR~v2.2: description and first results, Geoscientific Model Development, 10, 271–319, https://doi.org/10.5194/gmd-10-271-2017, 2017a.

Gasser, T., Peters, G. P., Fuglestvedt, J. S., Collins, W. J., Shindell, D. T., and Ciais, P.: Accounting for the climate-carbon feedback in emission metrics, Earth System Dynamics, 8, 235–253, https://doi.org/10.5194/esd-8-235-2017, 2017b.

Gasser, T., Kechiar, M., Ciais, P., Burke, E. J., Kleinen, T., Zhu, D., Huang, Y., Ekici, A., and Obersteiner, M.: Path-dependent reductions in CO2 emission budgets caused by permafrost carbon release, Nature Geoscience, 11, 830–835, https://doi.org/10.1038/s41561-018-0227-0, 2018.

Geoffroy, O., Saint-Martin, D., Olivié, D. J. L., Voldoire, A., Bellon, G., and Tytéca, S.: Transient Climate Response in a Two-Layer Energy-Balance Model. Part I: Analytical Solution and Parameter Calibration Using CMIP5 AOGCM Experiments, Journal of Climate, 26, 1841–1857, https://doi.org/10.1175/jcli-d-12-00195.1, 2013.

Ghan, S. J., Smith, S. J., Wang, M., Zhang, K., Pringle, K., Carslaw, K., Pierce, J., Bauer, S., and Adams, P.: A simple model of global aerosol indirect effects, Journal of Geophysical Research: Atmospheres, 118, 6688–6707, https://doi.org/10.1002/jgrd.50567, 2013.

Gidden, M. and Huppmann, D.: pyam: a Python Package for the Analysis and Visualization of Models of the Interaction of Climate, Human, and Environmental Systems, Journal of Open Source Software, 4, 1095, https://doi.org/10.21105/joss.01095, 2019.

Gidden, M. J., Riahi, K., Smith, S. J., Fujimori, S., Luderer, G., Kriegler, E., van Vuuren, D. P., van den Berg, M., Feng, L., Klein, D., Calvin, K., Doelman, J. C., Frank, S., Fricko, O., Harmsen, M., Hasegawa, T., Havlik, P., Hilaire, J., Hoesly, R., Horing, J., Popp, A., Stehfest, E., and Takahashi, K.: Global emissions pathways under different socioeconomic scenarios for use in CMIP6: a dataset of harmonized emissions trajectories through the end of the century, Geoscientific Model Development, 12, 1443–1475, https://doi.org/10.5194/gmd-12-1443-2019, 2019.

Gillett, N. P., Shiogama, H., Funke, B., Hegerl, G., Knutti, R., Matthes, K., Santer, B. D., Stone, D., and Tebaldi, C.: The Detection and Attribution Model Intercomparison Project (DAMIP~v1.0) contribution to CMIP6, Geoscientific Model Development, 9, 3685–3697, https://doi.org/10.5194/gmd-9-3685-2016, 2016.

Goodwin, P.: How historic simulation–observation discrepancy affects future warming projections in a very large model ensemble, Climate Dynamics, 47, 2219–2233, https://doi.org/10.1007/s00382-015-2960-z, 2016.

Goodwin, P.: On the Time Evolution of Climate Sensitivity and Future Warming, Earth's Future, 6, 1336–1348, https://doi.org/10.1029/2018ef000889, 2018.

Goodwin, P., Williams, R. G., and Ridgwell, A.: Sensitivity of climate to cumulative carbon emissions due to compensation of ocean heat and carbon uptake, Nature Geoscience, 8, 29–34, https://doi.org/10.1038/ngeo2304, 2014.

Goodwin, P., Katavouta, A., Roussenov, V. M., Foster, G. L., Rohling, E. J., and Williams, R. G.: Pathways to 1.5 °C and 2 °C warming based on observational and geological constraints, Nature Geoscience, 11, 102–107, https://doi.org/10.1038/s41561-017-0054-8, 2018.

Goodwin, P., Williams, R. G., Roussenov, V. M., and Katavouta, A.: Climate Sensitivity From Both Physical and Carbon Cycle Feedbacks, Geophysical Research Letters, 46, 7554–7564, https://doi.org/10.1029/2019gl082887, 2019.

Gregory, J. M.: A new method for diagnosing radiative forcing and climate sensitivity, Geophysical Research Letters, 31, https://doi.org/10.1029/2003gl018747, 2004.

https://doi.org/10.5194/gmd-2019-375
Preprint. Discussion started: 21 January 2020

Gütschow, J., Jeffery, M. L., Gieseke, R., Gebel, R., Stevens, D., Krapp, M., and Rocha, M.: The PRIMAP-hist national historical emissions time series, Earth System Science Data, 8, 571–603, https://doi.org/10.5194/essd-8-571-2016, https://doi.org/10.5194/essd-8-571-2016, 2016.

Hansen, J.: Efficacy of climate forcings, Journal of Geophysical Research, 110, https://doi.org/10.1029/2005jd005776, 2005.

Harmsen, M. J. H. M., van Vuuren, D. P., van den Berg, M., Hof, A. F., Hope, C., Krey, V., Lamarque, J.-F., Marcucci, A., Shindell, D. T., and Schaeffer, M.: How well do integrated assessment models represent non-CO2 radiative forcing?, Climatic Change, 133, 565–582, https://doi.org/10.1007/s10584-015-1485-0, 2015.

Hartin, C. A., Patel, P., Schwarber, A., Link, R. P., and Bond-Lamberty, B. P.: A simple object-oriented and open-source model for scientific and policy analyses of the global climate system – Hector v1.0, Geoscientific Model Development, 8, 939–955, https://doi.org/10.5194/gmd-8-939-2015, 2015.

Hawkins, E. and Sutton, R.: Connecting Climate Model Projections of Global Temperature Change with the Real World, Bulletin of the American Meteorological Society, 97, 963–980, https://doi.org/10.1175/bams-d-14-00154.1, 2016.

Held, I. M., Winton, M., Takahashi, K., Delworth, T., Zeng, F., and Vallis, G. K.: Probing the Fast and Slow Components of Global Warming by Returning Abruptly to Preindustrial Forcing, Journal of Climate, 23, 2418–2427, https://doi.org/10.1175/2009jcli3466.1, 2010.

Hoesly, R. M., Smith, S. J., Feng, L., Klimont, Z., Janssens-Maenhout, G., Pitkanen, T., Seibert, J. J., Vu, L., Andres, R. J., Bolt, R. M., Bond, T. C., Dawidowski, L., Kholod, N., Kurokawa, J.-i., Li, M., Liu, L., Lu, Z., Moura, M. C. P., O'Rourke, P. R., and Zhang, Q.: Historical (1750–2014) anthropogenic emissions of reactive gases and aerosols from the Community Emissions Data System (CEDS), Geoscientific Model Development, 11, 369–408, https://doi.org/10.5194/gmd-11-369-2018, https://doi.org/10.5194/gmd-11-369-2018, 2018.

Holmes, C. D., Prather, M. J., Søvde, O. A., and Myhre, G.: Future methane, hydroxyl, and their uncertainties: key climate and emission parameters for future predictions, Atmospheric Chemistry and Physics, 13, 285–302, https://doi.org/10.5194/acp-13-285-2013, 2013.

Hooss, G., Voss, R., Hasselmann, K., Maier-Reimer, E., and Joos, F.: A nonlinear impulse response model of the coupled carbon cycle-climate system (NICCS), Climate Dynamics, 18, 189–202, https://doi.org/10.1007/s003820100170, 2001.

Houghton, J. T., Meira Filho, L. G., Griggs, D. J., and Maskell, K.: An introduction to simple climate models used in the IPCC Second Assessment Report, Cambridge University Press Cambridge, http://large.stanford.edu/courses/2015/ph240/girard1/docs/houghton.pdf, 1997.

IPCC: Summary for Policymakers, book section SPM, p. 1–30, Cambridge University Press, Cambridge, United Kingdom and New York, NY, USA, https://doi.org/10.1017/CBO9781107415324.004, http://www.climatechange2013.org, 2013.

Jain, A., Wuebbles, D., and Kheshgi, H.: Integrated science model for assessment of climate change, Tech. rep., Lawrence Livermore National Lab., CA (United States), 1994.

Jones, C. D., Frölicher, T. L., Koven, C., MacDougall, A. H., Matthews, H. D., Zickfeld, K., Rogelj, J., Tokarska, K. B., Gillett, N. P., Ilyina, T., Meinshausen, M., Mengis, N., Séférian, R., Eby, M., and Burger, F. A.: The Zero Emissions Commitment Model Intercomparison Project (ZECMIP) contribution to C4MIP: quantifying committed climate changes following zero carbon emissions, Geoscientific Model Development, 12, 4375–4385, https://doi.org/10.5194/gmd-12-4375-2019, https://www.geosci-model-dev.net/12/4375/2019/, 2019.

Joos, F., Bruno, M., Fink, R., Siegenthaler, U., Stocker, T. F., Quéré, C. L., and Sarmiento, J. L.: An efficient and accurate representation of complex oceanic and biospheric models of anthropogenic carbon uptake, Tellus B: Chemical and Physical Meteorology, 48, 394–417, https://doi.org/10.3402/tellusb.v48i3.15921, 1996.

Joos, F., Roth, R., Fuglestvedt, J. S., Peters, G. P., Enting, I. G., von Bloh, W., Brovkin, V., Burke, E. J., Eby, M., Edwards, N. R., Friedrich, T., Frölicher, T. L., Halloran, P. R., Holden, P. B., Jones, C., Kleinen, T., Mackenzie, F. T., Matsumoto, K., Meinshausen, M., Plattner, G.-K., Reisinger, A., Segschneider, J., Shaffer, G., Steinacher, M., Strassmann, K., Tanaka, K., Timmermann, A., and Weaver, A. J.: Carbon

https://doi.org/10.5194/gmd-2019-375
Preprint. Discussion started: 21 January 2020

dioxide and climate impulse response functions for the computation of greenhouse gas metrics: a multi-model analysis, Atmospheric Chemistry and Physics, 13, 2793–2825, https://doi.org/10.5194/acp-13-2793-2013, 2013.

Kageyama, M., Braconnot, P., Harrison, S. P., Haywood, A. M., Jungclaus, J. H., Otto-Bliesner, B. L., Peterschmitt, J.-Y., Abe-Ouchi, A., Albani, S., Bartlein, P. J., Brierley, C., Crucifix, M., Dolan, A., Fernandez-Donado, L., Fischer, H., Hopcroft, P. O., Ivanovic, R. F., Lambert, F., Lunt, D. J., Mahowald, N. M., Peltier, W. R., Phipps, S. J., Roche, D. M., Schmidt, G. A., Tarasov, L., Valdes, P. J., Zhang, Q., and Zhou, T.: The PMIP4 contribution to CMIP6 – Part 1: Overview and over-arching analysis plan, Geoscientific Model Development, 11, 1033–1057, https://doi.org/10.5194/gmd-11-1033-2018, https://www.geosci-model-dev.net/11/1033/2018/, 2018.

Kriegler, E.: Imprecise probability analysis for integrated assessment of climate change, doctoralthesis, Universität Potsdam, https://publishup.uni-potsdam.de/opus4-ubp/frontdoor/index/index/docId/497, 2005.

Leach, N. J., Millar, R. J., Haustein, K., Jenkins, S., Graham, E., and Allen, M. R.: Current level and rate of warming determine emissions budgets under ambitious mitigation, Nature Geoscience, 11, 574, 2018.

Lee, Y. H., Lamarque, J.-F., Flanner, M. G., Jiao, C., Shindell, D. T., Berntsen, T., Bisiaux, M. M., Cao, J., Collins, W. J., Curran, M., Edwards, R., Faluvegi, G., Ghan, S., Horowitz, L. W., McConnell, J. R., Ming, J., Myhre, G., Nagashima, T., Naik, V., Rumbold, S. T., Skeie, R. B., Sudo, K., Takemura, T., Thevenon, F., Xu, B., and Yoon, J.-H.: Evaluation of preindustrial to present-day black carbon and its albedo forcing from Atmospheric Chemistry and Climate Model Intercomparison Project (ACCMIP), Atmospheric Chemistry and Physics, 13, 2607–2634, https://doi.org/10.5194/acp-13-2607-2013, 2013.

Meinshausen, M., Meinshausen, N., Hare, W., Raper, S. C. B., Frieler, K., Knutti, R., Frame, D. J., and Allen, M. R.: Greenhouse-gas emission targets for limiting global warming to 2 °C, Nature, 458, 1158–1162, https://doi.org/10.1038/nature08017, 2009.

Meinshausen, M., Raper, S. C. B., and Wigley, T. M. L.: Emulating coupled atmosphere-ocean and carbon cycle models with a simpler model, MAGICC6 – Part 1: Model description and calibration, Atmospheric Chemistry and Physics, 11, 1417–1456, https://doi.org/10.5194/acp-11-1417-2011, 2011a.

Meinshausen, M., Smith, S. J., Calvin, K., Daniel, J. S., Kainuma, M. L. T., Lamarque, J.-F., Matsumoto, K., Montzka, S. A., Raper, S. C. B., Riahi, K., Thomson, A., Velders, G. J. M., and van Vuuren, D. P.: The RCP greenhouse gas concentrations and their extensions from 1765 to 2300, Climatic Change, 109, 213–241, https://doi.org/10.1007/s10584-011-0156-z, https://doi.org/10.1007/s10584-011-0156-z, 2011b.

Meinshausen, M., Wigley, T. M. L., and Raper, S. C. B.: Emulating atmosphere-ocean and carbon cycle models with a simpler model, MAGICC6 – Part 2: Applications, Atmospheric Chemistry and Physics, 11, 1457–1471, https://doi.org/10.5194/acp-11-1457-2011, 2011c.

Meinshausen, M., Nicholls, Z., Lewis, J., Gidden, M. J., Vogel, E., Freund, M., Beyerle, U., Gessner, C., Nauels, A., Bauer, N., Canadell, J. G., Daniel, J. S., John, A., Krummel, P., Luderer, G., Meinshausen, N., Montzka, S. A., Rayner, P., Reimann, S., Smith, S. J., van den Berg, M., Velders, G. J. M., Vollmer, M., and Wang, H. J.: The SSP greenhouse gas concentrations and their extensions to 2500, https://doi.org/10.5194/gmd-2019-222, 2019.

Melton, J. R., Wania, R., Hodson, E. L., Poulter, B., Ringeval, B., Spahni, R., Bohn, T., Avis, C. A., Beerling, D. J., Chen, G., Eliseev, A. V., Denisov, S. N., Hopcroft, P. O., Lettenmaier, D. P., Riley, W. J., Singarayer, J. S., Subin, Z. M., Tian, H., Zürcher, S., Brovkin, V., van Bodegom, P. M., Kleinen, T., Yu, Z. C., and Kaplan, J. O.: Present state of global wetland extent and wetland methane modelling: conclusions from a model inter-comparison project (WETCHIMP), Biogeosciences, 10, 753–788, https://doi.org/10.5194/bg-10-753-2013, 2013.

https://doi.org/10.5194/gmd-2019-375
Preprint. Discussion started: 21 January 2020

Millar, R. J., Nicholls, Z. R., Friedlingstein, P., and Allen, M. R.: A modified impulse-response representation of the global near-surface air temperature and atmospheric concentration response to carbon dioxide emissions, Atmospheric Chemistry and Physics, 17, 7213–7228, https://doi.org/10.5194/acp-17-7213-2017, 2017.

Morice, C. P., Kennedy, J. J., Rayner, N. A., and Jones, P. D.: Quantifying uncertainties in global and regional temperature change using an ensemble of observational estimates: The HadCRUT4 data set, Journal of Geophysical Research: Atmospheres, 117, n/a–n/a, https://doi.org/10.1029/2011jd017187, 2012.

Myhre, G., Samset, B. H., Schulz, M., Balkanski, Y., Bauer, S., Berntsen, T. K., Bian, H., Bellouin, N., Chin, M., Diehl, T., Easter, R. C., Feichter, J., Ghan, S. J., Hauglustaine, D., Iversen, T., Kinne, S., Kirkevåg, A., Lamarque, J.-F., Lin, G., Liu, X., Lund, M. T., Luo, G., Ma, X., van Noije, T., Penner, J. E., Rasch, P. J., Ruiz, A., Seland, Ø., Skeie, R. B., Stier, P., Takemura, T., Tsigaridis, K., Wang, P., Wang, Z., Xu, L., Yu, H., Yu, F., Yoon, J.-H., Zhang, K., Zhang, H., and Zhou, C.: Radiative forcing of the direct aerosol effect from AeroCom Phase II simulations, Atmospheric Chemistry and Physics, 13, 1853–1877, https://doi.org/10.5194/acp-13-1853-2013, 2013a.

Myhre, G., Shindell, D., Bréon, F.-M., Collins, W., Fuglestvedt, J., Huang, J., Koch, D., Lamarque, J.-F., Lee, D., Mendoza, B., Nakajima, T., Robock, A., Stephens, G., Takemura, T., and Zhang, H.: Anthropogenic and Natural Radiative Forcing, book section 8, p. 659–740, Cambridge University Press, Cambridge, United Kingdom and New York, NY, USA, https://doi.org/10.1017/CBO9781107415324.018, http://www.climatechange2013.org, 2013b.

Nauels, A., Meinshausen, M., Mengel, M., Lorbacher, K., and Wigley, T. M. L.: Synthesizing long-term sea level rise projections – the MAGICC sea level model v2.0, Geoscientific Model Development, 10, 2495–2524, https://doi.org/10.5194/gmd-10-2495-2017, 2017.

Newman, P. A., Nash, E. R., Kawa, S. R., Montzka, S. A., and Schauffler, S. M.: When will the Antarctic ozone hole recover?, Geophysical Research Letters, 33, https://doi.org/10.1029/2005gl025232, 2006.

O'Neill, B. C., Tebaldi, C., van Vuuren, D. P., Eyring, V., Friedlingstein, P., Hurtt, G., Knutti, R., Kriegler, E., Lamarque, J.-F., Lowe, J., Meehl, G. A., Moss, R., Riahi, K., and Sanderson, B. M.: The Scenario Model Intercomparison Project (ScenarioMIP) for CMIP6, Geoscientific Model Development, 9, 3461–3482, https://doi.org/10.5194/gmd-9-3461-2016, 2016.

Prather, M. J., Hsu, J., DeLuca, N. M., Jackman, C. H., Oman, L. D., Douglass, A. R., Fleming, E. L., Strahan, S. E., Steenrod, S. D., Søvde, O. A., Isaksen, I. S. A., Froidevaux, L., and Funke, B.: Measuring and modeling the lifetime of nitrous oxide including its variability, Journal of Geophysical Research: Atmospheres, 120, 5693–5705, https://doi.org/10.1002/2015jd023267, 2015.

Pugh, T. A. M., Jones, C. D., Huntingford, C., Burton, C., Arneth, A., Brovkin, V., Ciais, P., Lomas, M., Robertson, E., Piao, S. L., and Sitch, S.: A Large Committed Long-Term Sink of Carbon due to Vegetation Dynamics, Earth's Future, 6, 1413–1432, https://doi.org/10.1029/2018ef000935, 2018.

Quéré, C. L., Andrew, R. M., Canadell, J. G., Sitch, S., Korsbakken, J. I., Peters, G. P., Manning, A. C., Boden, T. A., Tans, P. P., Houghton, R. A., Keeling, R. F., Alin, S., Andrews, O. D., Anthoni, P., Barbero, L., Bopp, L., Chevallier, F., Chini, L. P., Ciais, P., Currie, K., Delire, C., Doney, S. C., Friedlingstein, P., Gkritzalis, T., Harris, I., Hauck, J., Haverd, V., Hoppema, M., Goldewijk, K. K., Jain, A. K., Kato, E., Körtzinger, A., Landschützer, P., Lefèvre, N., Lenton, A., Lienert, S., Lombardozzi, D., Melton, J. R., Metzl, N., Millero, F., Monteiro, P. M. S., Munro, D. R., Nabel, J. E. M. S., Nakaoka, S.-i., O'Brien, K., Olsen, A., Omar, A. M., Ono, T., Pierrot, D., Poulter, B., Rödenbeck, C., Salisbury, J., Schuster, U., Schwinger, J., Séférian, R., Skjelvan, I., Stocker, B. D., Sutton, A. J., Takahashi, T., Tian, H., Tilbrook, B., van der Laan-Luijkx, I. T., van der Werf, G. R., Viovy, N., Walker, A. P., Wiltshire, A. J., and Zaehle, S.: Global Carbon Budget 2016, Earth System Science Data, 8, 605–649, https://doi.org/10.5194/essd-8-605-2016, https://doi.org/10.5194/essd-8-605-2016, 2016.

Quéré, C. L., Andrew, R. M., Friedlingstein, P., Sitch, S., Hauck, J., Pongratz, J., Pickers, P. A., Korsbakken, J. I., Peters, G. P., Canadell, J. G., Arneth, A., Arora, V. K., Barbero, L., Bastos, A., Bopp, L., Chevallier, F., Chini, L. P., Ciais, P., Doney, S. C., Gkritzalis, T., Goll,

https://doi.org/10.5194/gmd-2019-375
Preprint. Discussion started: 21 January 2020

D. S., Harris, I., Haverd, V., Hoffman, F. M., Hoppema, M., Houghton, R. A., Hurtt, G., Ilyina, T., Jain, A. K., Johannessen, T., Jones, C. D., Kato, E., Keeling, R. F., Goldewijk, K. K., Landschützer, P., Lefèvre, N., Lienert, S., Liu, Z., Lombardozzi, D., Metzl, N., Munro, D. R., Nabel, J. E. M. S., Nakaoka, S.-i., Neill, C., Olsen, A., Ono, T., Patra, P., Peregon, A., Peters, W., Peylin, P., Pfeil, B., Pierrot, D., Poulter, B., Rehder, G., Resplandy, L., Robertson, E., Rocher, M., Rödenbeck, C., Schuster, U., Schwinger, J., Séférian, R., Skjelvan, I., Steinhoff, T., Sutton, A., Tans, P. P., Tian, H., Tilbrook, B., Tubiello, F. N., van der Laan-Luijkx, I. T., van der Werf, G. R., Viovy, N., Walker, A. P., Wiltshire, A. J., Wright, R., Zaehle, S., and Zheng, B.: Global Carbon Budget 2018, Earth System Science Data, 10, 2141–2194, https://doi.org/10.5194/essd-10-2141-2018, 2018.

Randers, J., Golüke, U., Wenstøp, F., and Wenstøp, S.: A user-friendly earth system model of low complexity: the ESCIMO system dynamics model of global warming towards 2100, Earth System Dynamics, 7, 831–850, https://doi.org/10.5194/esd-7-831-2016, 2016.

Ravishankara, A. R., Daniel, J. S., and Portmann, R. W.: Nitrous Oxide (N2O): The Dominant Ozone-Depleting Substance Emitted in the 21st Century, Science, 326, 123–125, https://doi.org/10.1126/science.1176985, 2009.

Reddy, M. S. and Boucher, O.: Climate impact of black carbon emitted from energy consumption in the world's regions, Geophysical Research Letters, 34, https://doi.org/10.1029/2006gl028904, 2007.

Richardson, M., Cowtan, K., Hawkins, E., and Stolpe, M. B.: Reconciled climate response estimates from climate models and the energy budget of Earth, Nature Climate Change, 6, 931–935, https://doi.org/10.1038/nclimate3066, 2016.

Rogelj, J., Forster, P. M., Kriegler, E., Smith, C. J., and Séférian, R.: Estimating and tracking the remaining carbon budget for stringent climate targets, Nature, 571, 335–342, https://doi.org/10.1038/s41586-019-1368-z, 2019.

Rohrschneider, T., Stevens, B., and Mauritsen, T.: On simple representations of the climate response to external radiative forcing, Climate Dynamics, 53, 3131–3145, https://doi.org/10.1007/s00382-019-04686-4, 2019.

Schlesinger, M. E., Jiang, X., and Charlson, R. J.: Implication of Anthropogenic Atmospheric Sulphate for the Sensitivity of the Climate System, in: Climate Change and Energy Policy: Proceedings of the International Conference on Global Climate Change: Its Mitigation Through Improved Production and Use of Energy, edited by Rosen, L. and Glasser, R., pp. 75–108, American Institute of Physics, 1992.

Schwarber, A. K., Smith, S. J., Hartin, C. A., Vega-Westhoff, B. A., and Sriver, R.: Evaluating climate emulation: fundamental impulse testing of simple climate models, Earth System Dynamics, 10, 729–739, https://doi.org/10.5194/esd-10-729-2019, 2019.

Siegenthaler, U. and Joos, F.: Use of a simple model for studying oceanic tracer distributions and the global carbon cycle, Tellus B, 44, 186–207, https://doi.org/10.1034/j.1600-0889.1992.t01-2-00003.x, https://doi.org/10.1034%2Fj.1600-0889.1992.t01-2-00003.x, 1992.

Sitch, S., Friedlingstein, P., Gruber, N., Jones, S. D., Murray-Tortarolo, G., Ahlström, A., Doney, S. C., Graven, H., Heinze, C., Huntingford, C., Levis, S., Levy, P. E., Lomas, M., Poulter, B., Viovy, N., Zaehle, S., Zeng, N., Arneth, A., Bonan, G., Bopp, L., Canadell, J. G., Chevallier, F., Ciais, P., Ellis, R., Gloor, M., Peylin, P., Piao, S. L., Quéré, C. L., Smith, B., Zhu, Z., and Myneni, R.: Recent trends and drivers of regional sources and sinks of carbon dioxide, Biogeosciences, 12, 653–679, https://doi.org/10.5194/bg-12-653-2015, 2015.

Skeie, R. B., Fuglestvedt, J., Berntsen, T., Peters, G. P., Andrew, R., Allen, M., and Kallbekken, S.: Perspective has a strong effect on the calculation of historical contributions to global warming, Environmental Research Letters, 12, 024 022, https://doi.org/10.1088/1748-9326/aa5b0a, 2017.

Skeie, R. B., Berntsen, T., Aldrin, M., Holden, M., and Myhre, G.: Climate sensitivity estimates – sensitivity to radiative forcing time series and observational data, Earth System Dynamics, 9, 879–894, https://doi.org/10.5194/esd-9-879-2018, 2018.

Smith, C. J., Forster, P. M., Allen, M., Leach, N., Millar, R. J., Passerello, G. A., and Regayre, L. A.: FAIR v1.3: a simple emissions-based impulse response and carbon cycle model, Geoscientific Model Development, 11, 2273–2297, https://doi.org/10.5194/gmd-11-2273-2018, 2018a.

https://doi.org/10.5194/gmd-2019-375
Preprint. Discussion started: 21 January 2020

Smith, C. J., Kramer, R. J., Myhre, G., Forster, P. M., Soden, B. J., Andrews, T., Boucher, O., Faluvegi, G., Fläschner, D., Hodnebrog, Ø., Kasoar, M., Kharin, V., Kirkevåg, A., Lamarque, J.-F., Mülmenstädt, J., Olivié, D., Richardson, T., Samset, B. H., Shindell, D., Stier, P., Takemura, T., Voulgarakis, A., and Watson-Parris, D.: Understanding Rapid Adjustments to Diverse Forcing Agents, Geophysical Research Letters, 45, 12,023–12,031, https://doi.org/10.1029/2018GL079826, https://agupubs.onlinelibrary.wiley.com/doi/abs/10.1029/2018GL079826, 2018b.

Smith, C. J., Gieseke, R., and Nicholls, Z.: OMS-NetZero/FAIR: RCMIP phase 1, https://doi.org/10.5281/ZENODO.3588880, https://zenodo.org/record/3588880, 2019.

Stassen, C., Dommenget, D., and Loveday, N.: A hydrological cycle model for the Globally Resolved Energy Balance (GREB) model v1.0, Geoscientific Model Development, 12, 425–440, https://doi.org/10.5194/gmd-12-425-2019, 2019.

Stevens, B.: Rethinking the Lower Bound on Aerosol Radiative Forcing, Journal of Climate, 28, 4794–4819, https://doi.org/10.1175/jcli-d-14-00656.1, 2015.

Stevenson, D. S., Young, P. J., Naik, V., Lamarque, J.-F., Shindell, D. T., Voulgarakis, A., Skeie, R. B., Dalsoren, S. B., Myhre, G., Berntsen, T. K., Folberth, G. A., Rumbold, S. T., Collins, W. J., MacKenzie, I. A., Doherty, R. M., Zeng, G., van Noije, T. P. C., Strunk, A., Bergmann, D., Cameron-Smith, P., Plummer, D. A., Strode, S. A., Horowitz, L., Lee, Y. H., Szopa, S., Sudo, K., Nagashima, T., Josse, B., Cionni, I., Righi, M., Eyring, V., Conley, A., Bowman, K. W., Wild, O., and Archibald, A.: Tropospheric ozone changes, radiative forcing and attribution to emissions in the Atmospheric Chemistry and Climate Model Intercomparison Project (ACCMIP), Atmospheric Chemistry and Physics, 13, 3063–3085, https://doi.org/10.5194/acp-13-3063-2013, 2013.

Tanaka, K. and O'Neill, B. C.: The Paris Agreement zero-emissions goal is not always consistent with the 1.5 °C and 2 °C temperature targets, Nature Climate Change, 8, 319–324, https://doi.org/10.1038/s41558-018-0097-x, 2018.

Tanaka, K., Kriegler, E., Bruckner, T., Hooss, G., Knorr, W., Raddatz, T., and Tol, R.: Aggregated Carbon cycle, atmospheric chemistry and climate model (ACC2): description of forward and inverse mode, https://pure.mpg.de/rest/items/item_994422/component/file_994421/content, 2007.

Tanaka, K., Raddatz, T., O'Neill, B. C., and Reick, C. H.: Insufficient forcing uncertainty underestimates the risk of high climate sensitivity, Geophysical Research Letters, 36, https://doi.org/10.1029/2009gl039642, 2009.

Taylor, K. E., Stouffer, R. J., and Meehl, G. A.: An Overview of CMIP5 and the Experiment Design, Bulletin of the American Meteorological Society, 93, 485–498, https://doi.org/10.1175/bams-d-11-00094.1, 2012.

Tsutsui, J.: Quantification of temperature response to CO2 forcing in atmosphere–ocean general circulation models, Climatic Change, 140, 287–305, https://doi.org/10.1007/s10584-016-1832-9, 2017.

Tsutsui, J.: Diagnosing transient response to CO2 forcing in coupled atmosphere-ocean model experiments using a climate model emulator, Submitted to Geophysical Research Letters.

van Marle, M. J. E., Kloster, S., Magi, B. I., Marlon, J. R., Daniau, A.-L., Field, R. D., Arneth, A., Forrest, M., Hantson, S., Kehrwald, N. M., Knorr, W., Lasslop, G., Li, F., Mangeon, S., Yue, C., Kaiser, J. W., and van der Werf, G. R.: Historic global biomass burning emissions for CMIP6 (BB4CMIP) based on merging satellite observations with proxies and fire models (1750–2015), Geoscientific Model Development, 10, 3329–3357, https://doi.org/10.5194/gmd-10-3329-2017, https://doi.org/10.5194/gmd-10-3329-2017, 2017.

van Vuuren, D. P., Lowe, J., Stehfest, E., Gohar, L., Hof, A. F., Hope, C., Warren, R., Meinshausen, M., and Plattner, G.-K.: How well do integrated assessment models simulate climate change?, Climatic Change, 104, 255–285, https://doi.org/10.1007/s10584-009-9764-2, 2011.

https://doi.org/10.5194/gmd-2019-375
Preprint. Discussion started: 21 January 2020

Vega-Westhoff, B., Sriver, R. L., Hartin, C. A., Wong, T. E., and Keller, K.: Impacts of Observational Constraints Related to Sea Level on Estimates of Climate Sensitivity, Earth's Future, 7, 677–690, https://doi.org/10.1029/2018ef001082, 2019.

Voldoire, A., Saint-Martin, D., Sénési, S., Decharme, B., Alias, A., Chevallier, M., Colin, J., Guérémy, J.-F., Michou, M., Moine, M.-P., Nabat, P., Roehrig, R., Salas y Mélia, D., Séférian, R., Valcke, S., Beau, I., Belamari, S., Berthet, S., Cassou, C., Cattiaux, J., Deshayes, J., Douville, H., Ethé, C., Franchistéguy, L., Geoffroy, O., Lévy, C., Madec, G., Meurdesoif, Y., Msadek, R., Ribes, A., Sanchez-Gomez, E., Terray, L., and Waldman, R.: Evaluation of CMIP6 DECK Experiments With CNRM-CM6-1, Journal of Advances in Modeling Earth Systems, 11, 2177–2213, https://doi.org/10.1029/2019MS001683, https://agupubs.onlinelibrary.wiley.com/doi/abs/10.1029/2019MS001683, 2019.

von Deimling, T. S., Meinshausen, M., Levermann, A., Huber, V., Frieler, K., Lawrence, D. M., and Brovkin, V.: Estimating the near-surface permafrost-carbon feedback on global warming, Biogeosciences, 9, 649–665, https://doi.org/10.5194/bg-9-649-2012, 2012.

Voosen, P.: New climate models forecast a warming surge, Science, 364, 222–223, https://doi.org/10.1126/science.364.6437.222, https://science.sciencemag.org/content/364/6437/222, 2019.

Wigley, T. M. L.: A simple inverse carbon cycle model, Global Biogeochemical Cycles, 5, 373–382, https://doi.org/10.1029/91gb02279, https://doi.org/10.1029%2F91gb02279, 1991.

Wigley, T. M. L. and Raper, S. C. B.: Thermal expansion of sea water associated with global warming, Nature, 330, 127–131, https://doi.org/10.1038/330127a0, https://doi.org/10.1038%2F330127a0, 1987.

Wigley, T. M. L. and Schlesinger, M. E.: Analytical solution for the effect of increasing CO2 on global mean temperature, Nature, 315, 649–652, https://doi.org/10.1038/315649a0, https://doi.org/10.1038%2F315649a0, 1985.

Willner, S. N., Hartin, C., and Gieseke, R.: pyhector: A Python interface for the simple climate model Hector, The Journal of Open Source Software, 2, 248, https://doi.org/10.21105/joss.00248, 2017.

Wyser, K., van Noije, T., Yang, S., von Hardenberg, J., O'Donnell, D., and Döscher, R.: On the increased climate sensitivity in the EC-Earth model from CMIP5 to CMIP6, Geoscientific Model Development Discussions, 2019, 1–13, https://doi.org/10.5194/gmd-2019-282, https://www.geosci-model-dev-discuss.net/gmd-2019-282/, 2019.

https://doi.org/10.5194/gmd-2019-375
Preprint. Discussion started: 21 January 2020

Table 1. Overview of the physical components of the models participating in RCMIP Phase 1.

Model (acronym used in figures)	Spatial resolution	Temporal resolution	Climate response to radiative forcing	Other components
ACC2 (ACC2-v4-2)	Global land/ocean	Annual	1D ocean heat diffusion (DOECLIM)	Land and ocean carbon cycle, ocean carbonate chemistry, parameterized atmospheric chemistry involving CH4, OH, NOx, CO, and VOC, radiative forcing of 29 halocarbons
AR5IR (ar5ir-2box, ar5ir-3box)	Global	Annual	Impulse response	None
CICERO-SCM (CICERO-SCM)	By hemisphere	Annual	Energy balance/upwelling diffusion model	Land and ocean carbon cycle
ESCIMO (ESCIMO)	Global	Annual	Conserved flows of carbon, heat, albedo, permafrost, biome and biomass change. Driven by GHG emissions, the rest is endogenous.	No complete water cycle, water is tracked as ocean, high and low clouds, ice (glacial, arctic, Greenland and Antarctic), and vapor.
FaIR (FaIR-v1-5)	Global	Annual	Modified impulse response	Simple ozone, aerosol, greenhouse gas and land use relationships from precursor emissions
GIR (GIR)	Global	Annual	Modified Impulse Response	Simple (typically state-dependent) ozone, aerosol and greenhouse gas relationships
GREB (GREB-v1-0-1)	96 x 48 grid	Monthly	Energy Balance model atmospheric transport of heat and moisture, surface and subsurface ocean layer.	Hydrological cycle, sea ice.
Hector (hector|62381e71)	Global	Annual	1D ocean heat diffusion (DOECLIM)	Land and ocean carbon cycle. Ocean carbonate chemistry and simplified thermohaline circulation. Atmospheric chemistry of CH4, OH, NOx, and halocarbons.
Held et. al two layer model (held-two-layer-uom)	Global	Monthly	Two-layer ocean with state-dependent climate feedback factor	None

Geoscientific Model Development Discussions
Open Access
EGU

https://doi.org/10.5194/gmd-2019-375
Preprint. Discussion started: 21 January 2020

Geoscientific Model Development Discussions
Open Access
EGU

Table 1. Continued.

Model (acronym used in figures)	Spatial resolution	Temporal resolution	Climate response to radiative forcing	Other components
MAGICC (MAGICC-v7-1-0-beta)	Land/ocean by hemisphere.	Annual	Atmospheric energy balance model with 50-layer upwelling-diffusion-entrainment ocean.	Carbon cycle, permafrost module, ozone, 42 greenhouse gas cycles, sea level rise.
MCE (MCE-v1-1)	Global	Flexible; typically annual or five-yearly	Impulse response	Land and ocean carbon cycle
OSCAR (OSCAR-v3-0)	Global, with regionalized land carbon cycle	annual	Impulse response	Ocean and land carbon cycle, book-keeping module for land-use, biomass burning, wetlands, permafrost, tropospheric and stratospheric chemistry, 37 halogenated compounds, aerosols
WASP (WASP-v2)	Global	Annual	Energy balance using time evolving climate feedback, with conservation of heat and carbon	Land and ocean carbon cycle. Ocean pH. Thermosteric and ice-melt sea level components available.

https://doi.org/10.5194/gmd-2019-375
Preprint. Discussion started: 21 January 2020

Geoscientific Model Development Discussions
Open Access
EGU

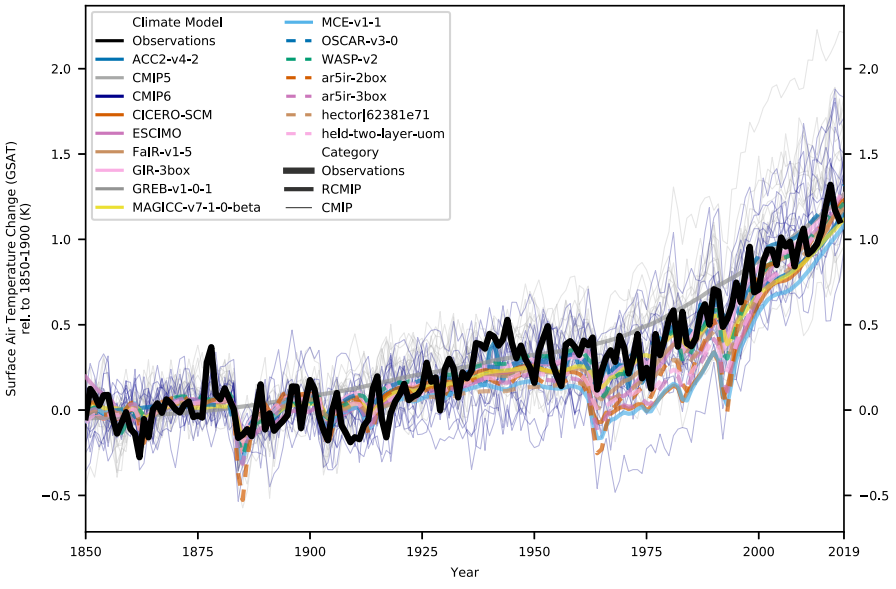

Figure 1. Historical global-mean annual mean surface air temperature (GSAT) simulations. Thick black line is observed GSAT (Richardson et al., 2016; Rogelj et al., 2019). Medium thickness lines are illustrative configurations for RCMIP models. Thin solid lines are CMIP models (CMIP6 in dark blue, CMIP5 in grey). In order to provide timeseries up until 2019, we have used data from the combination of historical and ssp585 simulations for RCMIP and CMIP6 models and rcp85 data for CMIP5 models.

https://doi.org/10.5194/gmd-2019-375
Preprint. Discussion started: 21 January 2020

Geoscientific Model Development Discussions
Open Access
EGU

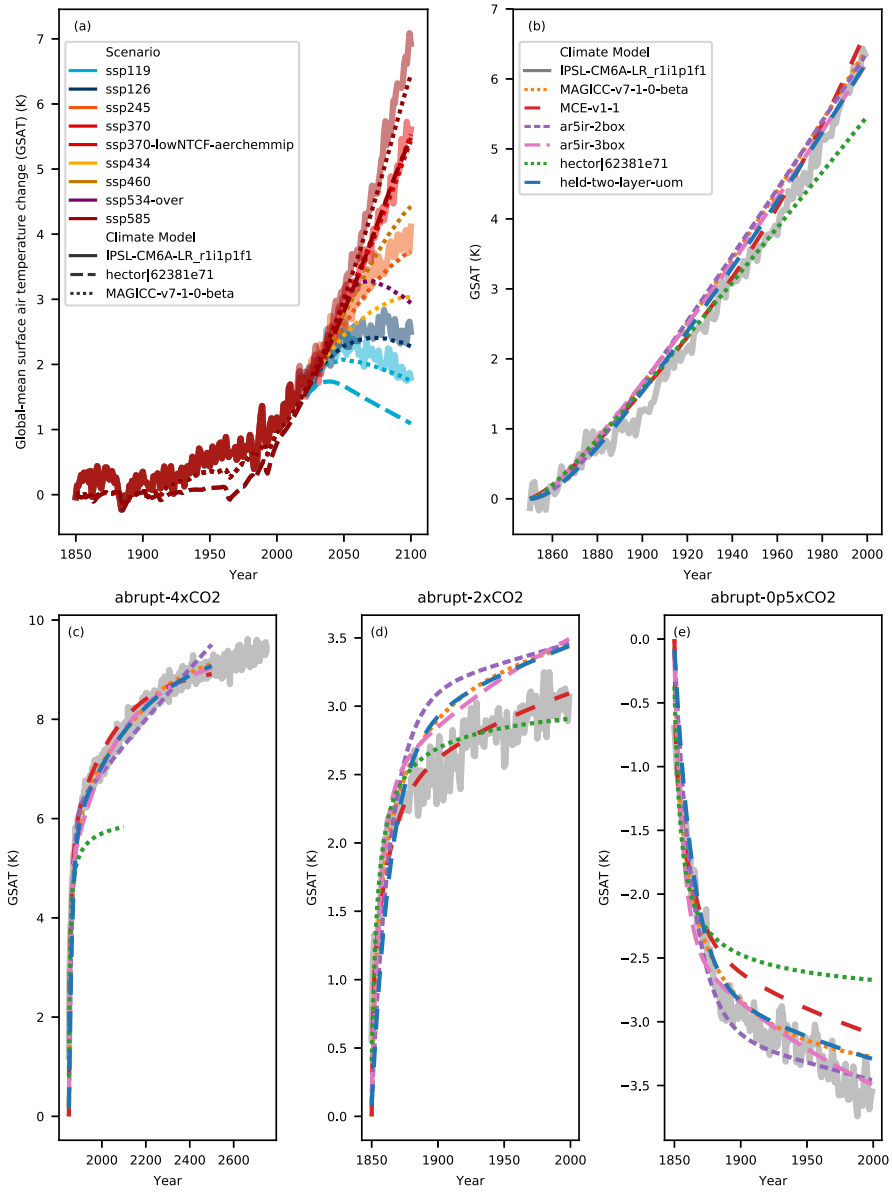

Figure 2. Emulation of CMIP6 models by RCMs. The thick transparent lines are the target CMIP6 model output (here from IPSL-CM6A-LR r1i1p1f1). The thin lines are emulations from different RCMs. Panel (a) shows results for scenario based experiments while panels (b) - (e) show results for idealised CO2-only experiments (note that panels (b) - (e) share the same legend). See the Supplementary Information for other target CMIP6 models.

https://doi.org/10.5194/gmd-2019-375
Preprint. Discussion started: 21 January 2020

Geoscientific Model Development Discussions
Open Access
EGU

Table 2. Model emulation scores over all emulated models and scenarios. Here we provide root-mean square errors over the SSPs plus four idealised CO2-only experiments (abrupt-2xCO2, abrupt-4xCO2, abrupt-0p5xCO2, 1pctCO2). As the models have not all provided emulations for the same set of models and scenarios, the model emulation scores are indicative only and are not a true, fair test of skill. For target model by target model emulation scores, see [TODO supplementary table reference].

Model (number of emulated scenarios)	**Surface Air Temperature Change (GSAT) i.e. tas**
hectorl62381e71 (32)	0.42 K
MCE-v1-1 (44)	0.19 K
MAGICC-v7-1-0-beta (135)	0.21 K
ar5ir-2box (40)	0.23 K
ar5ir-3box (40)	0.27 K
held-two-layer-uom (38)	0.17 K

https://doi.org/10.5194/gmd-2019-375
Preprint. Discussion started: 21 January 2020

Geoscientific Model Development Discussions
Open Access
EGU

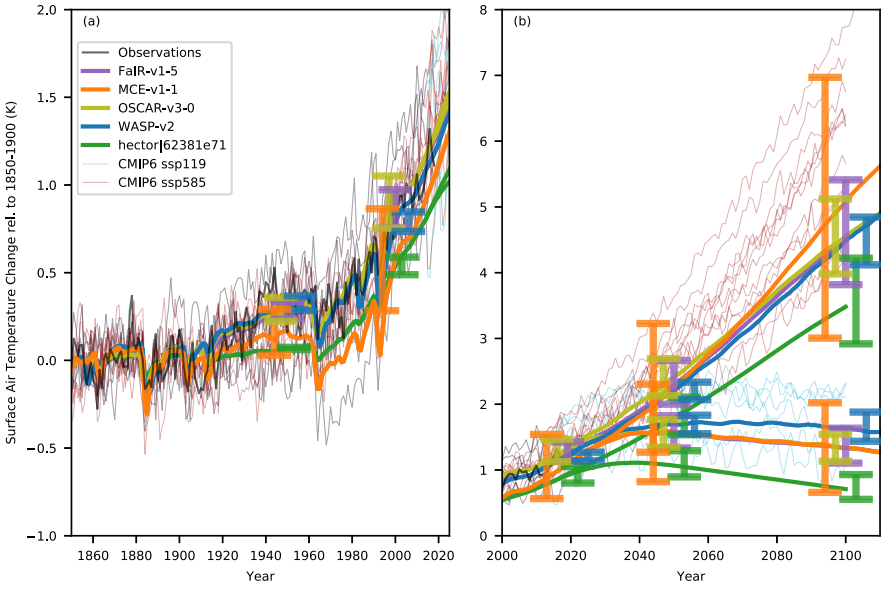

Figure 3. Probabilistic projections. Black line is observed GSAT (Richardson et al., 2016; Rogelj et al., 2019). Thick lines are RCMs (error bars represent 66% range) and thin lines are CMIP6 results. (a) - historical period (1850-2025); (b) - projections (2000-2110).

https://doi.org/10.5194/gmd-2019-375
Preprint. Discussion started: 21 January 2020

Geoscientific Model Development Discussions
Open Access
EGU

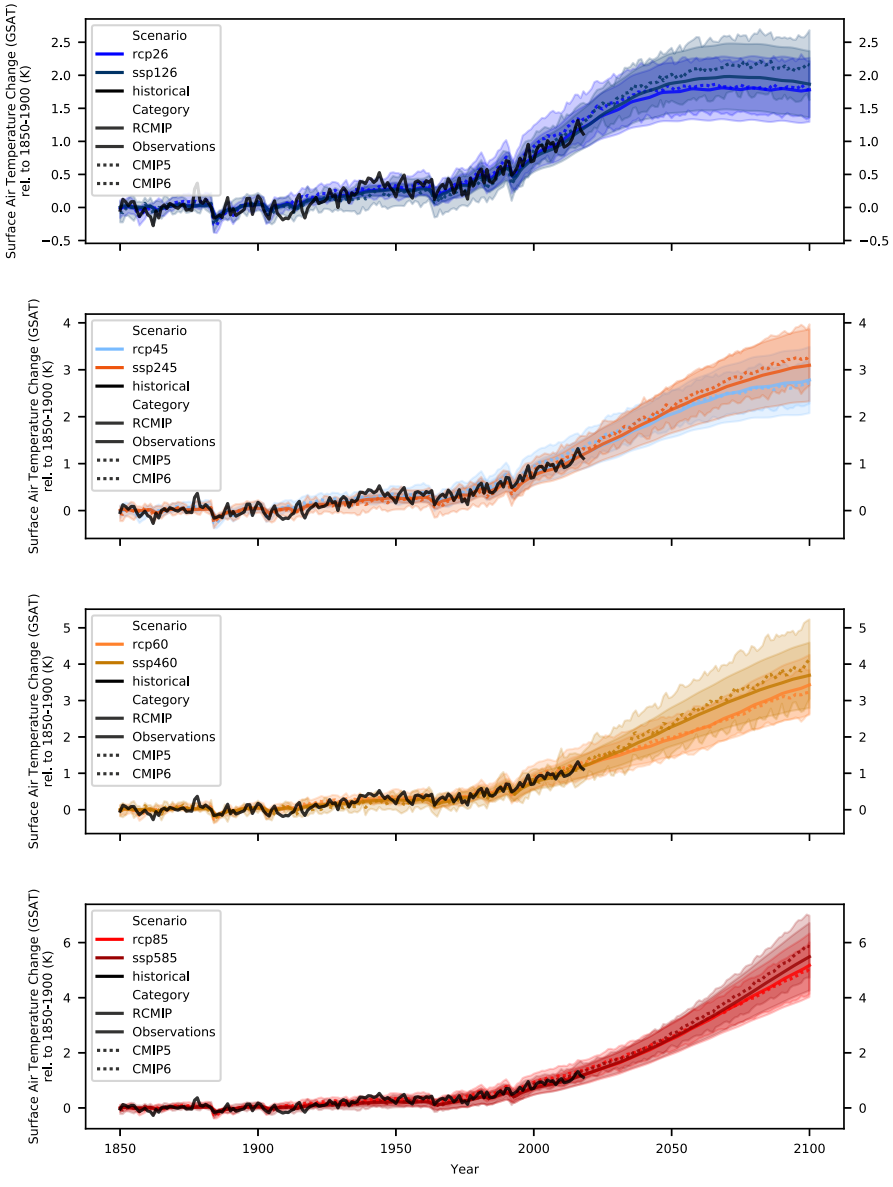

Figure 4. Comparison of temperature projections under the RCPs and SSPs up until 2100. The coloured solid lines are RCMIP output where the RCP/SSP pair has been run with the same model in the same configuration. For comparison, the dotted lines show CMIP5 and CMIP6 output. The plumes show one standard deviation of the available model results whilst the lines show the mean.